Journal Pre-proof

Discovery of novel cyclin-dependent kinase (CDK) and histone deacetylase (HDAC) dual inhibitors with potent *in vitro* and *in vivo* anticancer activity

Chunhui Cheng, Fan Yun, Sadeeq Ullah, Qipeng Yuan

PII: S0223-5234(20)30040-4

DOI: https://doi.org/10.1016/j.ejmech.2020.112073

Reference: EJMECH 112073

To appear in: *European Journal of Medicinal Chemistry*

Received Date: 9 December 2019

Revised Date: 3 January 2020

Accepted Date: 13 January 2020

Please cite this article as: C. Cheng, F. Yun, S. Ullah, Q. Yuan, Discovery of novel cyclin-dependent kinase (CDK) and histone deacetylase (HDAC) dual inhibitors with potent *in vitro* and *in vivo* anticancer activity, *European Journal of Medicinal Chemistry* (2020), doi: https://doi.org/10.1016/j.ejmech.2020.112073.

Graphic abstracts

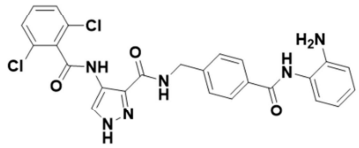

Compound 7c HDAC1, IC_{50}= 6.40nM
HDAC2, IC_{50}= 0.25nM
HDAC3, IC_{50}= 45.00nM
CDK1, IC_{50}= 8.63nM
CDK2, IC_{50}= 0.30nM

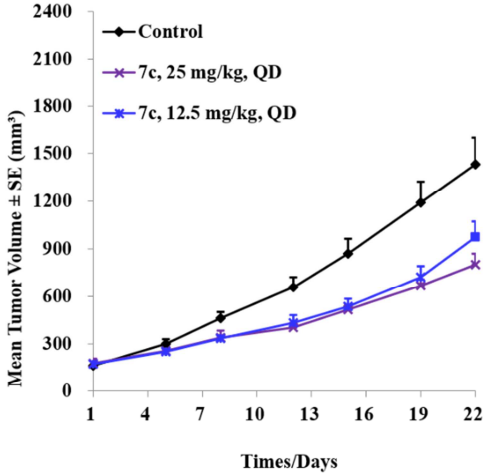

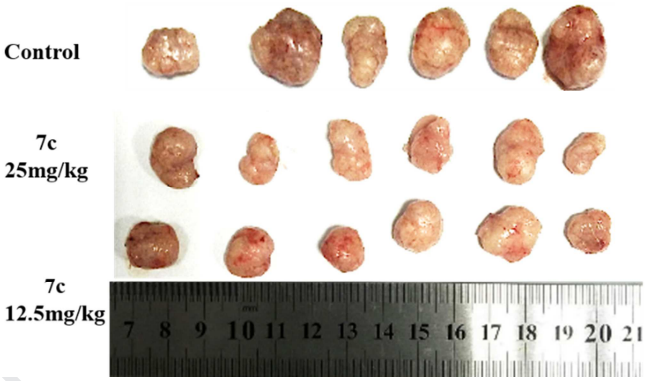

Discovery of Novel Cyclin-dependent Kinase (CDK) and Histone Deacetylase (HDAC) Dual Inhibitors with Potent *In Vitro* and *In Vivo* Anticancer Activity

Chunhui Cheng†, Fan Yun†, Sadeeq Ullah, Qipeng Yuan*

Key Laboratory of Biomedical Materials of Natural Macromolecules (Beijing University of Chemical Technology), Ministry of Education. College of Life Science and Technology, Beijing University of Chemical Technology, 15 Beisanhuan East Road, Beijing 100029, China

† These two authors contributed equally

*E-mail addresses of the corresponding authors: yuanqp@mail.buct.edu.cn

A B S T R A C T

In the current study, we reported a series of novel 1-H-pyrazole-3-carboxamide-based inhibitors targeting histone deacetylase (HDAC) and cyclin-dependent kinase (CDK). The representative compounds N-(4-((2-aminophenyl)carbamoyl)benzyl)-4-(2,6-dichlorobenzamido)-1H-pyrazole-3-carboxamide (**7c**) and N-(4-(2-((2-aminophenyl)amino)-2-oxoethyl)phenyl)-4-(2,6-dichlorobenzamido)-1H-pyrazole-3-carboxamide (**14a**) with potent antiproliferative activities towards five solid cancer cell lines, showed excellent inhibitory activities against HDAC2 (IC_{50} =0.25 and 0.24nM respectively) and CDK2 (IC_{50} =0.30 and 0.56nM respectively). In addition, compounds **7c** and **14a** significantly inhibited the migration of A375 and H460 cells. Further studies revealed that compounds **7c** and **14a** could arrest cell cycle in G2/M phase and promote apoptosis in A375, HCT116, H460 and Hela cells, which was associated with increasing the intracellular reactive oxygen species (ROS) levels. More importantly, compound **7c** possessed favorable pharmacokinetic properties with the intraperitoneal bioavailability of 63.6% in ICR mice, and potent *in vivo* antitumor efficacy in the HCT116 xenograft model. Our study demonstrated that compound **7c** provides a promising strategy for the treatment of malignant tumors.

Key words: **Histone deacetylase, Cyclin-dependent kinase, Antiproliferative activity, Pharmacokinetic properties, *In vivo* antitumor activity**

1 Introduction

Tumorigenesis is closely associated with gene mutations and abnormal chromosome modifications which are the category of epigenetic aberrations[1]. Histone deacetylases (HDACs) and histone acetyltransferases (HATs) are epigenetic enzymes, which jointly governed the acetylation of histone [2, 3]. Overexpressed HDACs could remove the acetyl group from the terminal lysine residues of histones, thus silencing the expression of tumor suppressor genes and resulting in tumor carcinoma[4-9]. HDAC inhibitors have received considerable success for cutaneous cell lymphoma therapy. Recently, four HDAC inhibitors, vorinostat (SAHA), romidepsin (FK228), belinostat (PXD-101), and panobinostat (LBH589) have been approved by U.S. Food and Drug Administration (FDA) for the therapy of hematological malignancies[10-13]. Chidamide (CS055) has been approved by China Food and Drug Administration for the treatment of peripheral T-cell lymphoma[14] (**Figure 1A**). Single HDAC inhibitors have been proved to be effective for the treatment of hematological malignancies, but they show low inhibitory activity against solid tumors[15, 16]. Moreover, many clinical researches have demonstrated that HDAC inhibitors exploit synergistic effects in combination with other anticancer agents[17-19]. However, multicomponent drugs raised the risks involved in complex pharmacokinetic properties, unpredictable drug-drug interactions and different drug solubilities[20, 21]. On the contrary, developing HDAC-based multitargeting drugs could provide an effective and practical strategy to overcome the limitations of single and multicomponent agents.

The dysfunction of cell cycle regulation is a remarkable future of the occurrence and development of malignant tumors[22]. Cyclin-dependent kinases (CDKs), belonging to a family of serine/threonine protein kinases, regulate cell cycle and promote cell growth, proliferation and apoptosis[23, 24]. To date, the CDK family have consisted of 20 members (CDK1-20), which form a CDK/ cyclin complex with associated cyclin to exert their function[25]. CDK1, 2, 4 and 6 play a crucial role in cell cycle, while CDK7, 8 and 9 are involved in transcriptional regulation[26, 27]. Abnormal expression of CDK2/cyclin A or CDK2/cyclin E leads to cell carcinoma, and overexpression of CDK2 induced by gene mutation has been identified in various human tumors, containing breast cancer, ovarian carcinoma, bladder cancer, endometrial carcinoma and gastric carcinoma[28-30]. As a consequence, CDK inhibitors have been considered as promising antineoplastic agents. So far, two CDK inhibitors have been approved by FDA: palbociclib[31] and ribociclib[32] for the treatment of breast cancer and HER2-negative advanced breast cancer respectively (**Figure 1B**). Several CDK inhibitors have been at different stages of clinical trials, for instance, (R)-roscovitine[33, 34], AT-7519[35] and flavopiridol[36, 37].

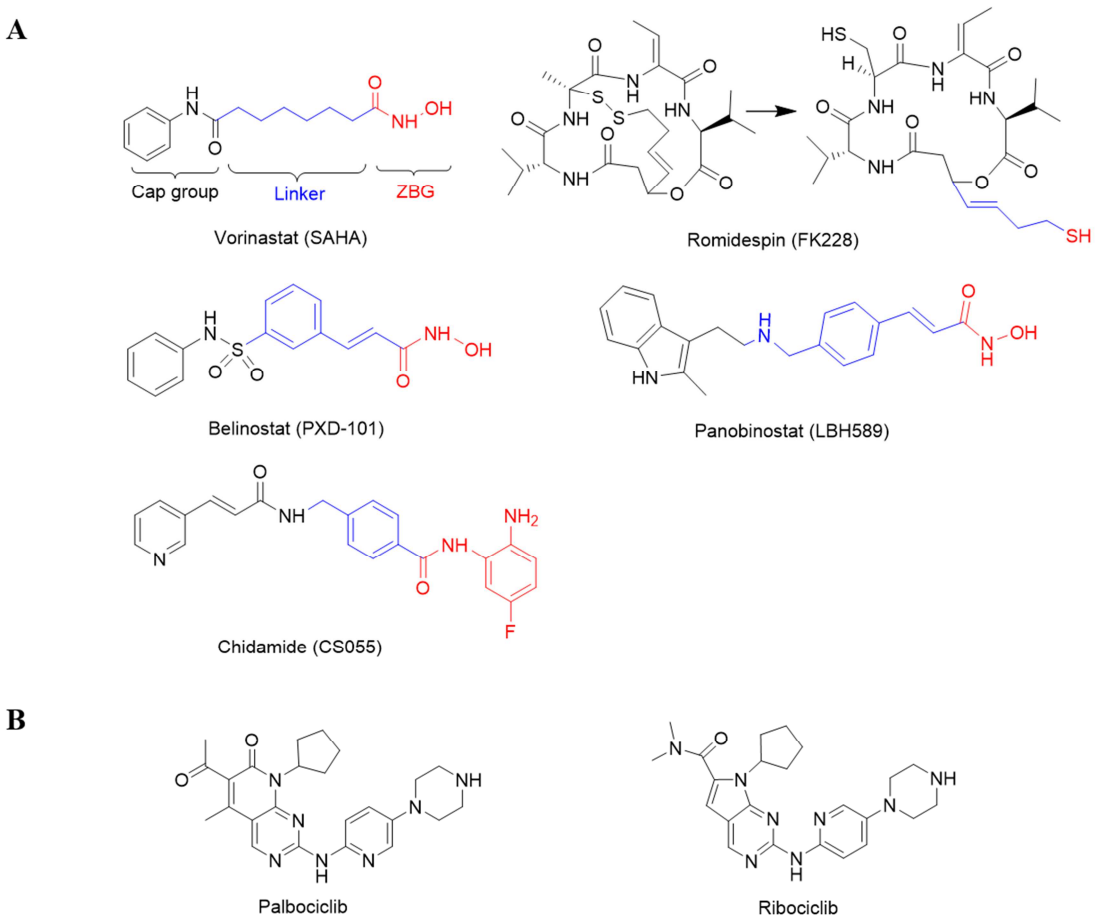

Fig.1. Chemical structures of approved HDAC (A) and CDK (B) inhibitors

It's reported that vorinostat and flavopiridol, a pan-CDK inhibitor, have synergized in leukemia, breast, lung and esophageal cancer[38, 39]. In addition, Fan et al. reported a series of novel CDK4/9 and HDAC1 dual inhibitors against malignant cancer[40]. These evidence indicated that designing rationally a multitargeting molecule inhibiting CDK and HDAC could be a promising strategy for cancer therapy. Compound **1**, 4-(2,6-difluorobenzamido)-N-(4-fluorophenyl)-1H-pyrazole-3-carboxamide, was proven to reveal high inhibitory activity against CDK1 and CDK2 enzymes, and good pharmacokinetic (PK) properties, indicating it to be a lead compound (**Figure 2**) [33, 35]. Additionally, pharmacophore models of most HDAC inhibitors comprise a cap group, a linker and a zinc-binding group (ZBG). The cap structure containing a hydrophobic ring interacts with amino acid residues at the protein surface; the linker occupies the tubular channel to connect the cap group and the zinc site; the zinc-binding group, such as hydroxamic acid and 2-aminobenzamide, chelates with zinc ion and forms hydrogen bonds in the catalytic site (**Figure 1**)[41, 42]. Considering that there is a large hydrophobic area on the surface of HDAC, we envisaged that the essential pharmacophore of compound **1** was merged with hydroxamic acid or *o*-aminobenzamide moiety to acquire a single molecule that could inhibit both HDAC as well as CDK enzymes. Furthermore, on basis of the strategy as

shown in **Figure 2** , we synthesized a series of dual CDK/ HDAC compounds, and evaluated their antitumor activity *in vitro* and *in vivo*.

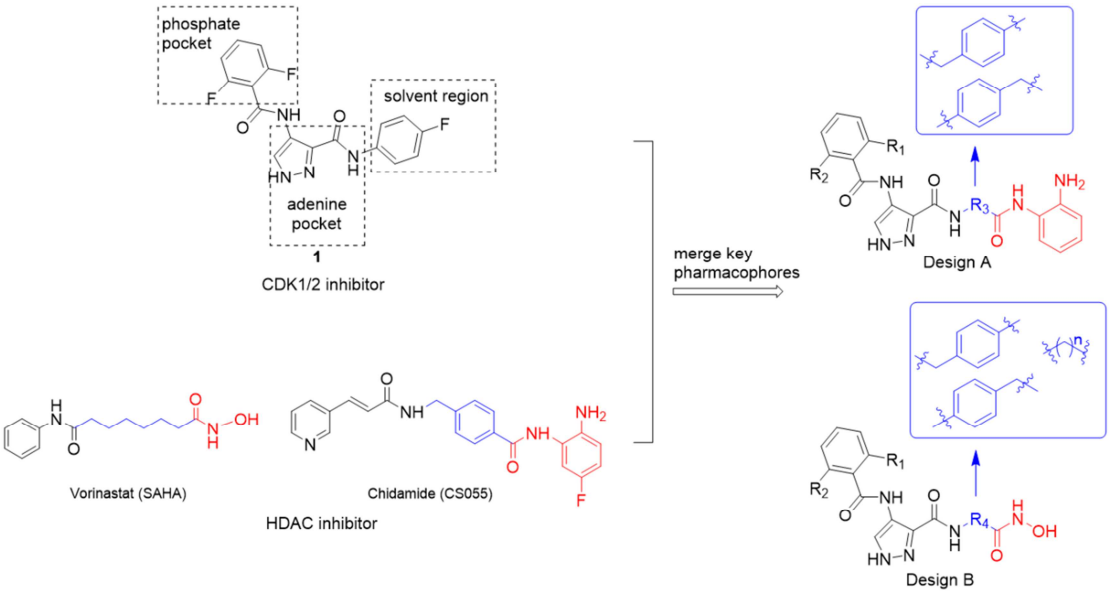

Fig.2. Design of multi-target inhibitors against HDAC and CDK.

2. Results and discussion

2.1 Chemistry

The synthetic routes of all target compounds were listed in **Scheme 1-3**. The preparation procedures of compounds **7a-7g** and **8a-8g** were illustrated in **Scheme 1**. Commercially available 4-nitro-1H-pyrazole-3-carboxylic acid (**2**) reacted with methyl 4-(aminomethyl)benzoate hydrochloride (**3**) to synthesize **4**, which was reduced by palladium on activated carbon to yield compound **5**. Then compound **5** was treated with different substituted benzoyl chlorides to afford the key intermediate **6**. The intermediate **6** was hydrolyzed, and then treated with benzene-1,2-diamine to give the target compounds **7a-7g**. In addition, the hydroxamic acids **8a-8g** were directly generated by compound **6** with fresh hydroxylamine solution.

As shown in **Scheme 2**, firstly, compound **10** was prepared by the reduction of methyl 4-nitro-1H-pyrazole-3-carboxylate (**9**) in the presence of palladium on activated carbon. **10** reacted with various benzoyl chlorides to afford compound **11**, which was subjected to hydrolysis in 1,4-dioxane to give the corresponding acid **12**. After that, the key intermediate **13** was obtained by **12** with ethyl 2-(4-aminophenyl)acetate. The synthesis of hydroxamic acids **15a-15g** was similar to that of **8a-8g**. Then target compounds **14a-14g** were prepared via the hydrolysis and condensation reaction from **13**. In **Scheme 3**, compound **12** was treated with available aminoalkylester hydrochlorides to provide the intermediate **16**, which was consequently converted to final products **17a-17g**.

Scheme 1. Synthesis of 7a-7g and 8a-8g [a]

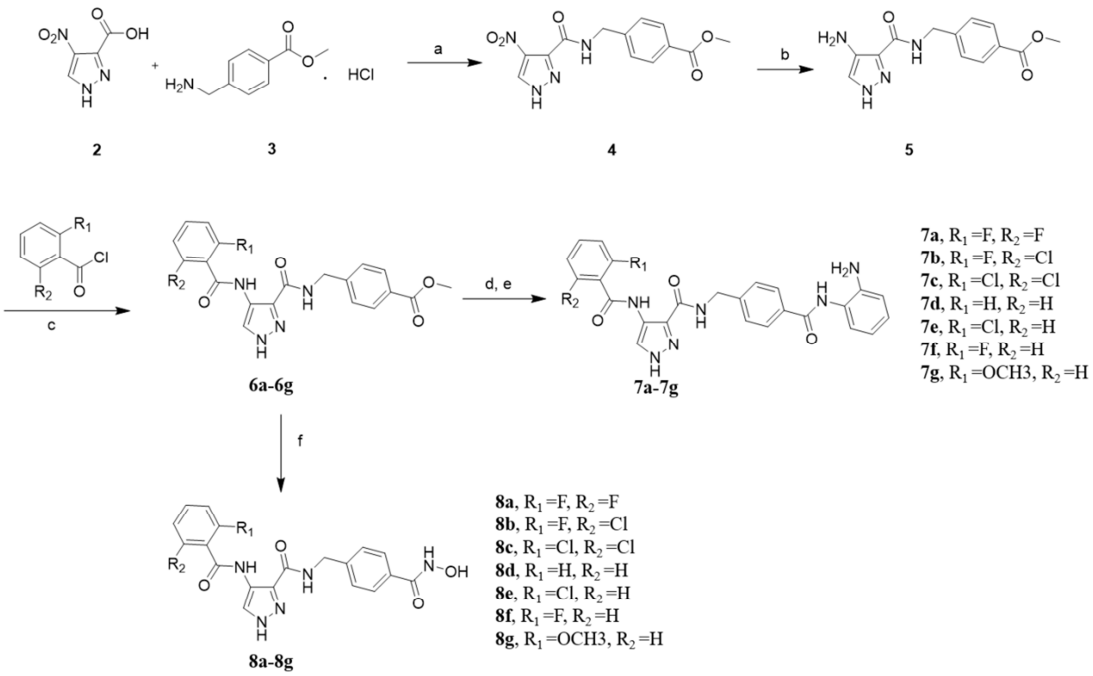

[a] Reagents and conditions: (a) EDCI, HOBt, DIEA, DMF, r.t; (b) Pd/C, $HCOONH_4$, THF: IPA=1:1, reflux; (c) corresponding benzoyl chlorides, triethylamine, 1,4-dioxane, 0□; (d) NaOH (4 equiv), 1,4-dioxane, 85□; (e) benzene-1,2-diamine, HBTU, TEA/DMF, r.t; (f) $NH_2OH·HCl$, KOH, MeOH, r.t.

Scheme 2 Synthesis of 14a-14g and 15a-15g [a]

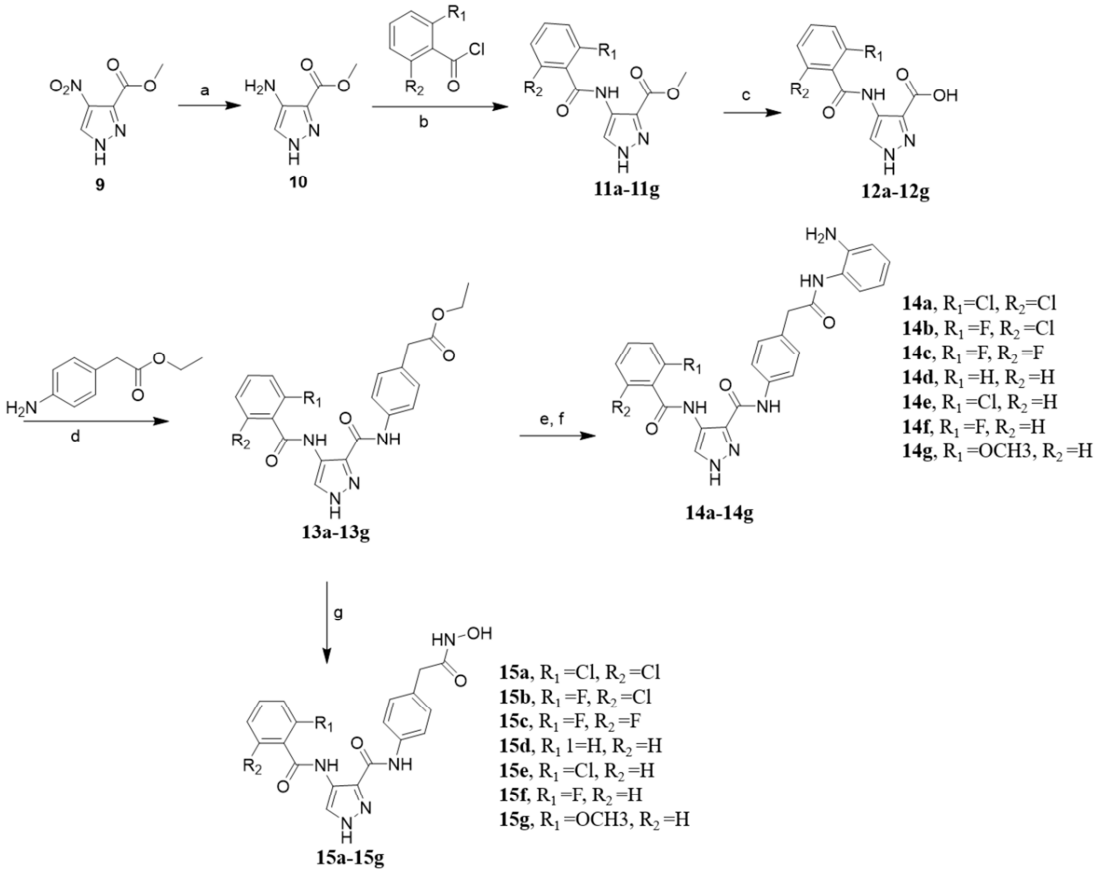

[a] Reagents and conditions: (a) Pd/C, $HCOONH_4$, THF: IPA=1:1, reflux; (b) corresponding benzoyl chlorides, triethylamine, 1,4-dioxane, 0□; (c) NaOH (4 equiv), 1,4-dioxane, 85□; (d) EDCI, HOBt, DIEA, DMF, r.t; (e) NaOH(4 equiv), 1,4-dioxane, 85□; (f) benzene-1,2-diamine, HBTU, TEA/DMF, r.t; (g) $NH_2OH·HCl$, KOH, MeOH, r.t.

Scheme 3 Synthesis of 17a-17g [a]

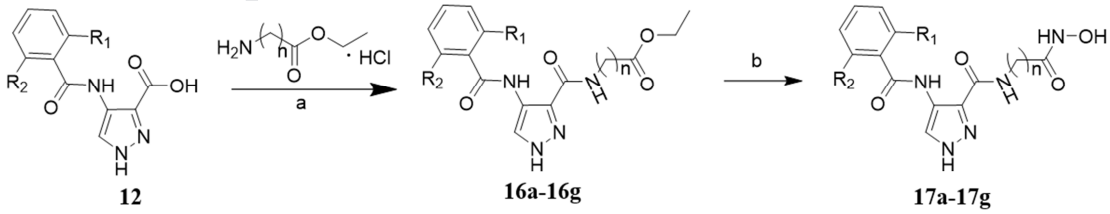

16a, R_1=Cl, R_2=Cl, n=6
16b, R_1=Cl, R_2=Cl, n=5
16c, R_1=F, R_2=F, n=6
16d, R_1=F, R_2=F, n=5
16e, R_1=F, R_2=F, n=4
16f, R_1=F, R_2=F, n=3
16g, R_1=F, R_2=Cl, n=6

17a, R_1=Cl, R_2=Cl, n=6
17b, R_1=Cl, R_2=Cl, n=5
17c, R_1=F, R_2=F, n=6
17d, R_1=F, R_2=F, n=5
17e, R_1=F, R_2=F, n=4
17f, R_1=F, R_2=F, n=3
17g, R_1=F, R_2=Cl, n=6

[a] Reagents and conditions: (a) EDCI, HOBt, DIEA, DMF, r.t; (b) $NH_2OH·HCl$, KOH, MeOH, r.t.

2.2 Biological evaluation

2.2.1 Assays of antiproliferative activity and enzyme inhibition

Table 1

Antiproliferative activity and enzyme inhibition data (inhib%) of the target compounds

	% cell growth inhibition [a]				% enzyme inhibition [a]	
	HCT116		H460		HDAC1	CDK2
Compd	8μM	2μM	8μM	2μM	10μM	10μM
7a	79.09%	73.12%	80.55%	13.92%	98.32%	66.84%
7b	83.75%	78.65%	75.01%	50.12%	90.41%	90.93%
7c	73.81%	73.77%	78.35%	32.83%	97.27%	82.99%
7d	88.61%	62.88%	61.71%	11.78%	96.71%	59.09%
7e	84.38%	63.73%	17.40%	5.54%	97.73%	53.61%
7f	81.19%	39.79%	57.57%	7.25%	97.50%	36.98%
7g	75.43%	23.52%	45.47%	5.73%	98.02%	97.18%
8a	64.49%	25.01%	7.33%	0.46%	72.58%	65.67%
8b	59.28%	46.24%	27.70%	10.37%	67.41%	53.21%
8c	81.91%	68.65%	57.40%	45.38%	80.73%	76.82%
8d	61.67%	29.41%	31.62%	11.99%	69.52%	51.26%
8e	71.61%	53.84%	29.84%	26.58%	98.69%	64.47%
8f	76.95%	51.01%	57.06%	23.54%	98.00%	76.14%
8g	68.78%	43.75%	45.64%	15.97%	79.18%	53.52%
14a	78.05%	72.88%	67.39%	57.33%	89.89%	95.83%
14b	74.29%	60.42%	75.06%	16.44%	85.12%	82.39%
14c	81.63%	76.80%	73.77%	3.52%	90.61%	91.88%
14d	69.20%	60.01%	8.93%	0.37%	78.15%	60.52%
14e	51.98%	29.17%	27.75%	3.08%	63.47%	41.71%
14f	20.42%	16.48%	23.37%	6.06%	41.29%	33.64%
14g	30.54%	13.63%	26.82%	3.12%	57.04%	11.34%
15a	75.81%	62.15%	75.06%	10.50%	94.22%	96.60%
15b	44.86%	21.70%	36.99%	12.46%	56.35%	44.35%
15c	25.56%	29.94%	30.18%	0.04%	44.97%	58.91%
15d	14.23%	9.56%	23.11%	11.82%	33.17%	7.65%
15e	4.52%	0.84%	26.56%	9.04%	24.51%	21.35%
15f	14.31%	1.04%	21.39%	9.50%	34.06%	22.42%
15g	24.51%	9.38%	24.25%	1.58%	46.14%	6.52%
17a	20.09%	1.07%	17.90%	16.96%	42.14%	35.83%
17b	4.66%	3.02%	21.31%	15.05%	24.32%	19.37%
17c	13.76%	12.08%	6.84%	3.57%	33.48%	27.52%
17d	59.41%	4.87%	28.77%	22.94%	70.13%	41.30%
17e	14.86%	5.76%	15.77%	0.40%	35.74%	45.79%
17f	6.54%	0.91%	25.32%	13.04%	26.82%	32.43%
17g	15.72%	10.01%	28.71%	0.88%	24.37%	12.28%
CS055	72.20%	64.43%	38.24%	1.73%	96.39%	-
SAHA	86.06%	77.79%	68.66%	26.05%	97.90%	-

1	73.97%	57.57%	59.13%	21.32%	-	66.61%

[a] The values represent the means of at least two separate experiments with SD less than 10%.

The results of antiproliferative activity and enzyme inhibition assays were displayed in **Table 1** with CS055, SAHA and compound **1** as the reference drugs. The growth inhibition of all compounds was examined at the concentrations of 8μM and 2μM towards human colorectal cancer cell line (HCT116) and human lung cancer cell line (H460). In addition, we also evaluated the enzyme inhibition for HDAC1 and CDK2 at 10μM. Compounds **17a-17g** with the long alkyl linker at the R_3 position significantly decreased the antiproliferative activity relative to those with the aromatic ring. The introduction of electron-donating methoxyl group (**7g**, **8g**, **14g** and **15g**) gave the weaker activity than that of electron-withdrawing groups, such as **7e**, **8e 14e** and **15e**. The *o*-aminobenzamide-based compounds **7b-7d** caused a remarkable increase of activity compared to **8b-8d** with hydroxamic acid as ZBG. Compounds **14a-14c**, simultaneously substituted with fluorine or chlorine moieties at the R_1 and R_2 positions exhibited better activity than those with R_2=H, such as **14d-14g**. Moreover, the antiproliferative activities were substantially consistent with enzyme inhibitory activities. For example, compounds **7a-8a** with higher cell growth inhibitory effects were also more effective against HDAC1 and CDK2 than compounds **15b-15f**.

HDACs or CDKs were overexpressed in many malignant tumors[43-48]. Particularly, it was reported that Class I HDACs showed aberrant upregulation in more than 75% tumor tissues[49, 50]. Studies have indicated that several novel CDK or HDAC inhibitors showed potent antiproliferative activity against human colorectal, lung, malignant, cervical and hepatoma cancer cell lines[51-60]. Consequently, IC_{50} values of compounds that revealed superior or similar antiproliferative activity to the positive controls were further investigated towards human cancer cell lines: HCT116, H460, A375, Hela and SMMC7721. As depicted in **Table 2**, compounds **7c** and **14a**, in which two chlorine atoms were linked at the R_1 and R_2 positions, exhibited excellent antiproliferative activities with IC_{50} values ranging from 0.71 to 7.76μM against five cell lines. Moreover, these two compounds were more potent for HCT116 cells (IC_{50} = 0.71 and 1.45μM, respectively) than CS055 (IC_{50} =2.77μM) and **1** (IC_{50} =1.96μM). The activity was weakened when R_1 was a fluorine atom and the R_2 position included fluorine or chlorine (**7b** and **7c**, IC_{50} from 0.70 to 16.26μM; **14b** and **14c**, IC_{50} from 2.57 to 16.46μM). These data clearly proved that the chlorine atoms at the R_1 and R_2 positions were the most optimal replacement, which illustrated that 2,6-dichlorobenzamide group was crucial to enhance the potency. However, most compounds showed poor cell inhibition towards SMMC7721 cells. In addition, compound **7c** was tested for the cell morphology at concentrations of 4, 1 and 0.25μM respectively against all cancer cells (**Figure 3**). The image analysis suggested that compounds could great change cell morphology while inhibiting cell growth.

Next, compounds **7c** and **14a** were tested in the mouse embryonic fibroblast cells NIH 3T3 to determine their effects on normal cells. As shown in **Table 3**, compounds

7c and **14a** exhibited low cytotoxicity with IC_{50} values of 4.47 and 4.64μM respectively compared with CS055 (IC_{50}= 2.46μM). Considering the antiproliferative activity and cytotoxicity, compounds **7c** and **14a** were evaluated for further biological activity.

Table 2

IC_{50} Values in 5 cancer cells of selected compounds

Compd	IC_{50}(μM) [a]				
	HCT116	A375	Hela	H460	SMMC7721
7a	1.13	1.70	4.48	7.79	15.21
7b	0.70	1.20	3.27	3.63	16.26
7c	0.71	1.20	1.83	4.19	7.76
7d	1.66	1.59	4.06	6.32	6.62
7e	0.90	2.11	10.47	6.36	12.93
7f	4.80	2.27	3.44	9.99	6.85
7g	3.68	2.66	8.13	7.35	8.32
8c	0.50	5.05	4.84	10.57	14.61
8e	2.40	6.42	16.20	6.17	21.78
8f	2.20	3.01	6.61	23.73	16.69
14a	1.45	1.60	3.15	2.63	5.22
14b	2.57	2.89	4.30	5.34	14.38
14c	3.46	2.97	8.89	4.99	16.46
15a	2.40	4.61	7.15	6.88	12.31
CS055	2.77	4.11	14.94	>32	25.59
SAHA	1.26	2.68	2.41	11.92	5.274
1	1.96	13.38	8.23	9.46	23.21

[a] Values are the means of at least two separate experiments.

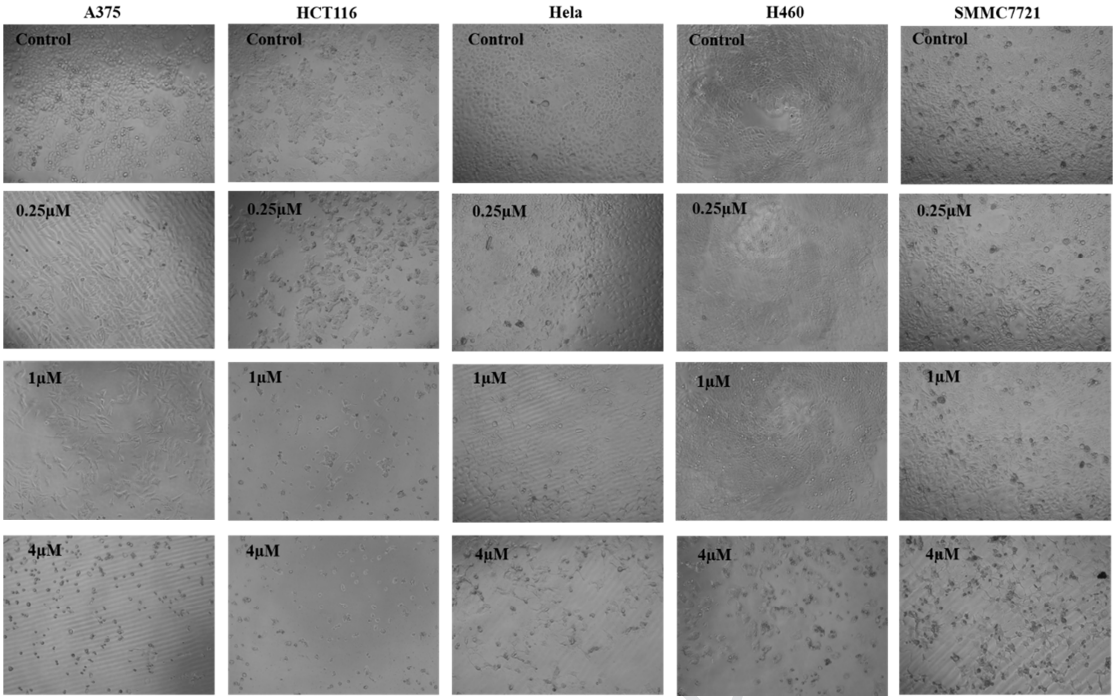

Figure 3. The human cancer cell lines were treated with **7c** at the indicated concentration or DMSO (0.1%) for 48 h, and the cells morphology was detected with microscope.

Table 3

Cytotoxicity against the NIH 3T3 normal cell line

Compd	**7c**	**14a**	**1**	CS055
NIN 3T3 IC_{50} (μM) [a]	4.47	4.64	7.85	2.46

[a] Values are the mean of three separate experiments

2.2.2 *In vitro* HDAC and CDK inhibitory activity assay

Compounds **7c** and **14a** were selected for *in vitro* inhibitory assays against HDACs and CDKs since these compounds showed high potency. It's evident from **Table 3** that compounds **7c** and **14a** revealed significant isoform selectivity for HDAC2 (IC_{50}= 0.25 and 0.24nM respectively) over other HDACs. Compound **7c** was above 40-fold and 4-fold more potent for HDAC1 and HDAC3 compared with CS055. Compound **14a** exhibited comparable HDAC1 inhibition to CS055, whereas for HDAC3, **14a** was less active with IC_{50} >1000nM. These two compounds have little inhibition effects on HDAC6 and HDAC8. In addition, among CDKs, compound **7c** and **14a** displayed higher inhibitory activity against CDK2 with IC_{50} values of 0.30 and 0.56nM respectively. It was noteworthy that these two compounds also had inhibitory activity against CDK1 (**7c**, IC_{50} = 8.63nM; **14a**, IC_{50} =12.58nM). The IC_{50} values of **7c** and **14a** towards other CDKs were >1000nM. From these results, we can confirm that compounds **7c** and **14a** possessed dual HDAC and CDK inhibitory activity.

Table 4

Inhibitory profile of compounds **7c** and **14a** against HDACs and CDKs

Compd	IC_{50} (nM) [a]						
	HDAC1	HDAC2	HDAC3	HDAC6,8	CDK1	CDK2	CDK4,6,7
CS055	260	23.00	180	>1000	-	-	-
1	-	-	-	-	29.47	9.52	>1000
7c	6.4	0.25	45	>1000	8.63	0.30	>1000
14a	240	0.24	>1000	>1000	12.58	0.56	>1000

[a] Values are the means of at least two separate determinations.

2.2.3 Molecular docking study

We successfully performed molecular docking studies to disclose the binding interactions of the representative compounds (**7c** and **14a**) with HDAC2 and CDK2. As we speculated, compounds **7c** and **14a** were approached to the narrow binding-site channel, and the 2- aminobenzamide moiety chelated with zinc ion at the bottom catalytic site of HDAC2 (**Figure S1A**and **S1C** in Supporting Information). It's observed that both compounds **7c** and **14a** could form four important hydrogen bonds with HIS145, HIS146, GLY154 and TYR308 in the HDAC2 active site (**Figure 4A** and **4C**). In addition, the compound **7c** formed two other hydrogen bonding interactions with ASP181 and PHE210, and the cap group of **14a** also formed one additional hydrogen bond with LEU276. It might explain the reason that the HDAC1 inhibitory activity of compound **7c** was superior to that of **14a**. Furthermore, the pyrazole-3-carboxamide group of the compounds **7c** and **14a** could form hydrogen bonds to the backbone residues GLU81 and LEU83 in the hinge area of CDK2, which was essential for CDK2 inhibitory effects of compounds. Besides, **7c** formed extra hydrogen bonding interaction with HIS84 (**Figure 4B**), while **14a** was able to form similar hydrogen bond with LYS89 (**Figure 4D**). The molecular docking results provided a valid explanation for the interactions of compounds (**7c** and **14a**) with HDAC2 and CDK2, and also unveiled the appropriate dual inhibitor design.

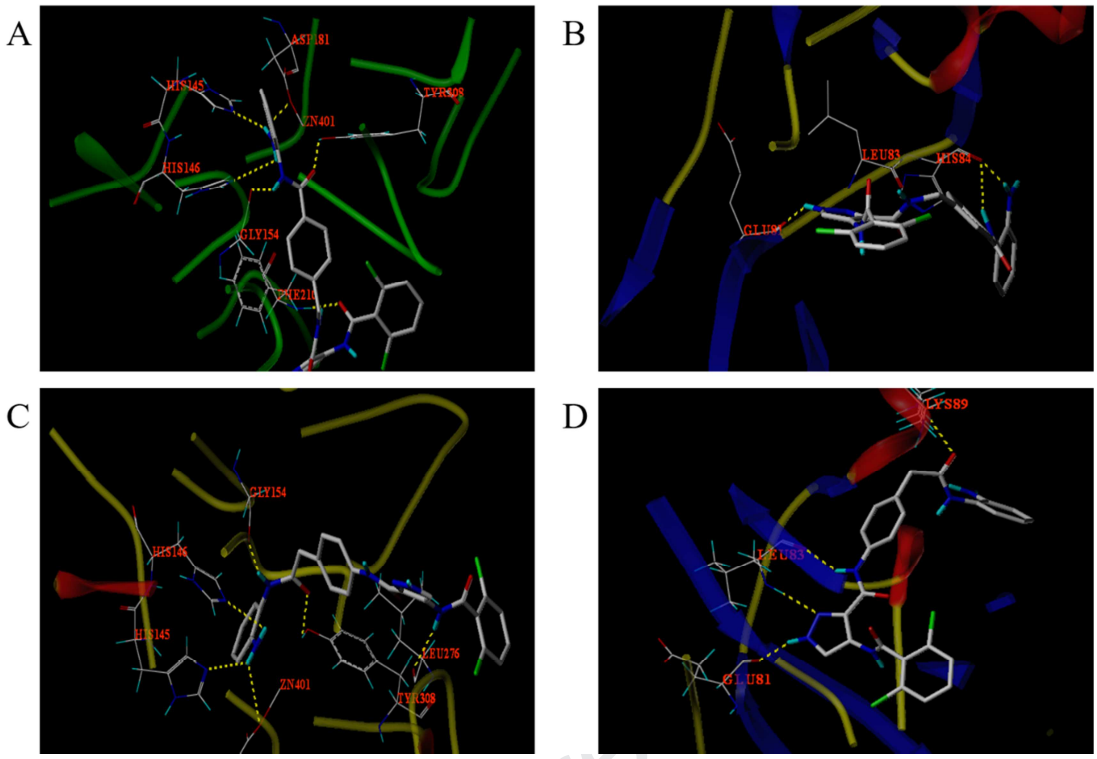

Figure 4. Predicted binding modes of compounds **7c** and **14a** with HDAC2 (PDB code: 4LXZ) and CDK2 (PDB code: 1PYE). Interactions between the protein and the ligand are shown as yellow dotted lines. (A) Predicted binding mode of compound **7c** in the active site of HDAC2. (B) Proposed binding mode of compound **7c** with CDK2. (C) Compound **14a** interacted with the active site of HDAC2. (D) Proposed binding mode of compound **14a** with CDK2. Protein surface of HDAC2 and CDK2 docking with compounds **7c** and **14a** was shown in the Supporting Information.

2.2.4 Cell scratch assay

Cell scratch assay is considered as an effective method to measure the cell migration and repair ability. To evaluate the inhibitory effect of the compounds on cells migration, A375 cells and H460 cells were cultured, and then treated with **7c**, **14a**, **1**, and CS055 for 48h. The images were mentioned in **Figure 5**. It's observed that A375 and H460 cells migration were apparently suppressed by **7c** and **14a** as compared to the positive controls **1** and CS055. The inhibitory ability of **14a** toward A375 cells migration was stronger than that of **7c**.

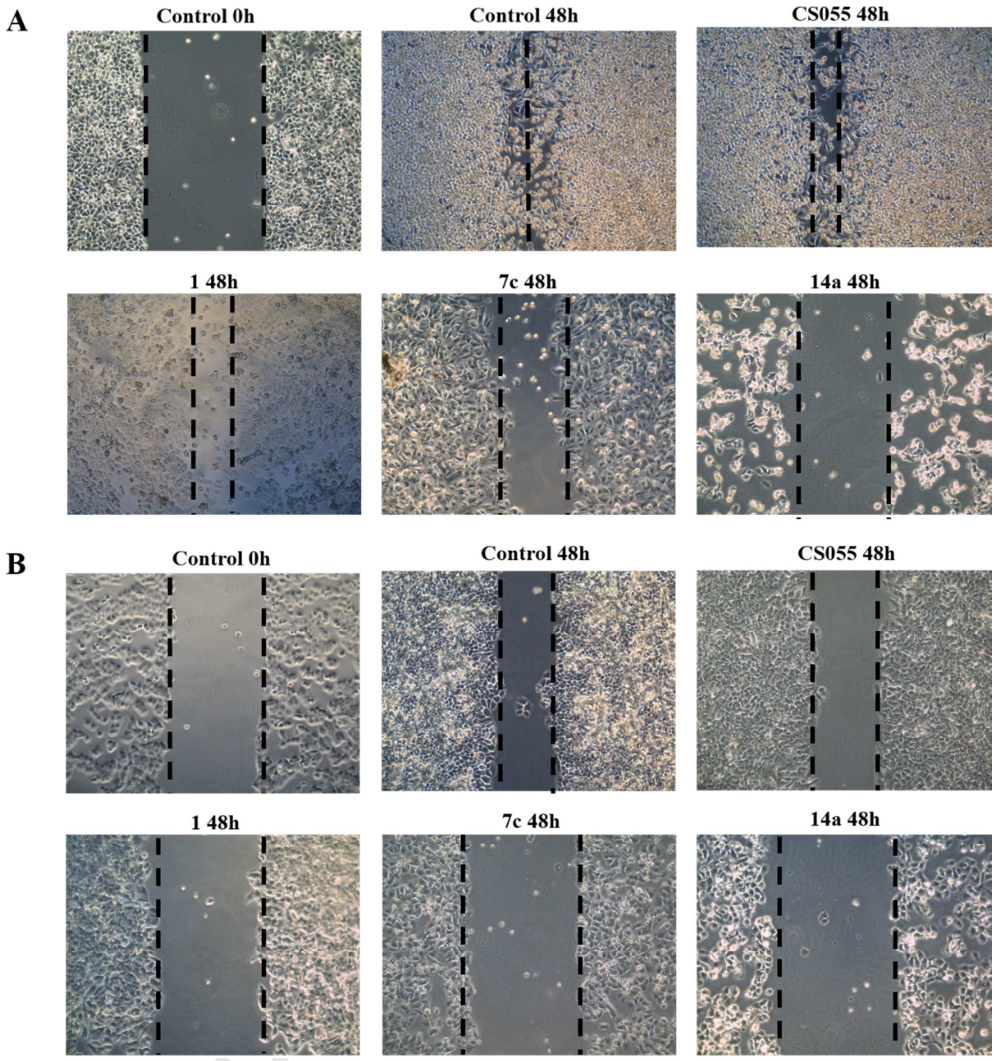

Figure 5. The effects of CS055, **1**, **7c** and **14a** on the migration of A375 cells (A) at 0.25μM and H460 cells (B) at 0.5μM. One representative of three independent experiments is shown.

2.2.5 Cell cycle analysis

To further explore the intracellular mechanisms of the representative compounds, **7c** and **14a** were carefully conducted for their cell cycle effects on A375 cell line, HCT116 cell line, H460 cell line and Hela cell line. Cells were treated with **7c** and **14a** at concentrations of 2, 1 and 0.5μM, as well as control (DMSO) for 24h, which were measured by the flow cytometry with propidium iodide (PI) staining. As presented in **Figure 6**, after treatment with **7c** and **14a,** cancer cells could show a loss in the proportion of cells in G0/G1 phase and an obvious increase in G2/M phase compared to control (DMSO). It's evidently observed that these compounds significantly arrested A375 and HCT116 cells in G2/M phase. For instance, the percentages of A375 cells for **7c** and **14a** at dose of 2μM were increased from 1.13% to 57.74% and 66.48% respectively (the data from **Figure S2** in Supporting Information). Taken together, the patterns of **7c** and **14a** blocking cell cycle were

consistent with that of compound **1**, which could be relevant to CDK2 inhibitory activity (**Figure S2** in Supporting Information).

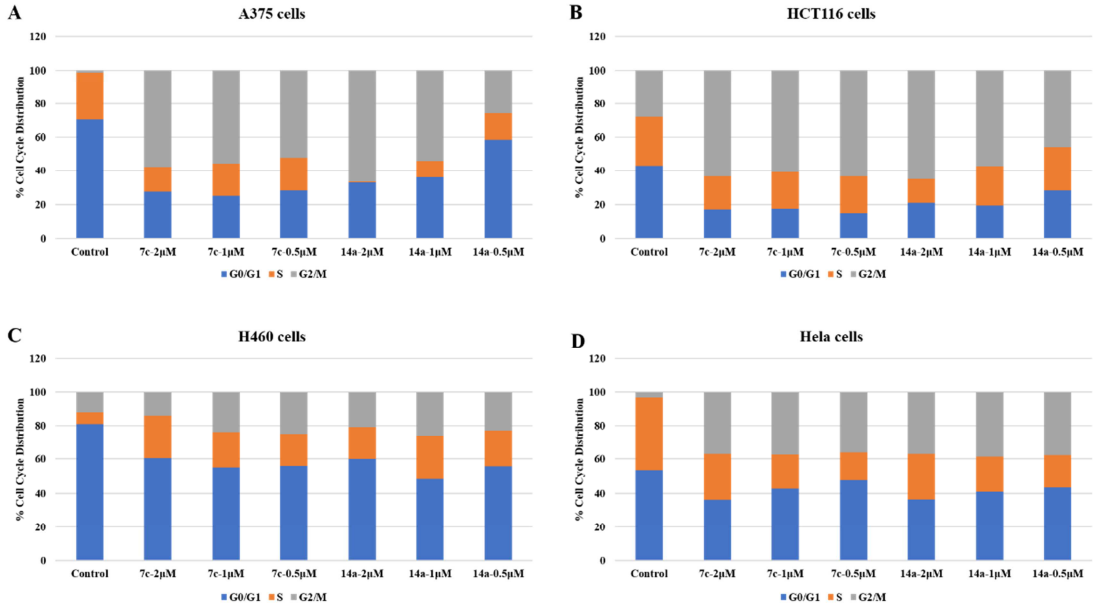

Figure 6. The effects of compounds **7c** and **14a** on the cell cycle assay of cancer cell lines. (A) A375 cell line; (B) HCT116 cell line; (C) H460 cell line; (D) Hela cell line.

2.2.6 Cell apoptosis assay

We next wanted to determine that the capacity of compounds **7c** and **14a** to induce cell death via apoptosis in A375 cell line, HCT116 cell line, H460 cell line and Hela cell line. Cells were treated with **7c** and **14a**, CS055 and compound **1** as the reference drugs for 48h, which were stained with FITC-Annexin V and propidium iodide (PI), and then analyzed by flow cytometry. **Figure 7** indicated that the compounds **7c** and **14a** could expedite cell apoptosis in a concentration-dependent manner. Compounds **7c** and **14a** could more effectively induce apoptosis than control (DMSO) towards all four cell lines. The apoptosis rates of **7c** and **14a** towards A375 cells were 97.22% and 73.08% respectively, which were higher than that of compound **1** (66.71%) and CS055 (62.60%) at the concentration of 2μM. The apoptosis rates of HCT116 cells induced by **7c** and **14a** were 60.6% and 77.1% respectively, however, compound **1** and CS055 induced 48.00% and 44.30% respectively. They showed stronger effects on cell apoptosis against A375 and HCT116 cells. For H460 and Hela cells, the apoptosis induced by **7c** and **14a** was better than that of CS055. Hence, it can be concluded that **7c** and **14a** could cause cell death through apoptosis.

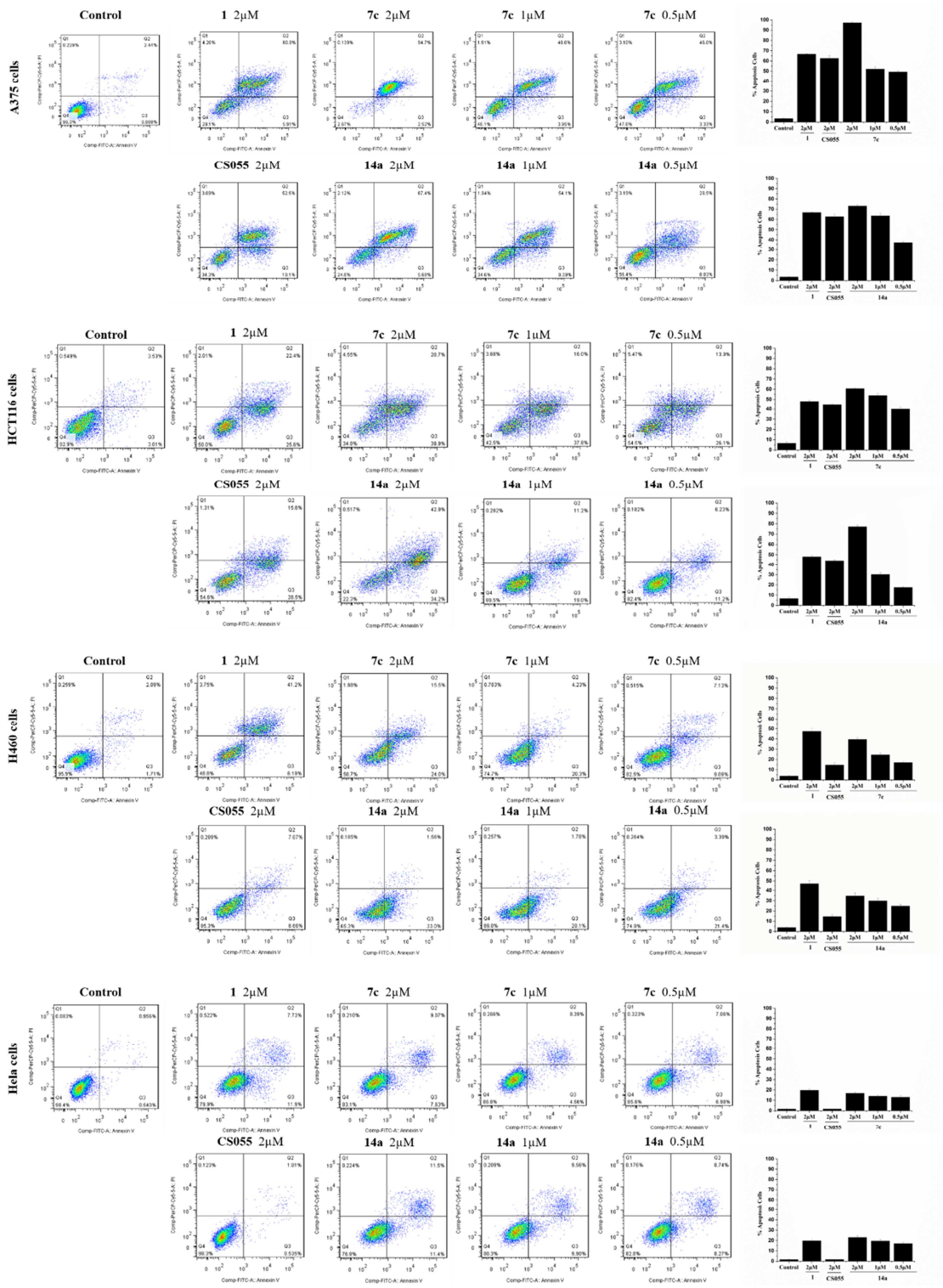

Figure 7. Effects of **7c** and **14a** on the apoptosis of cells. Cells were treated with compounds **7c**, **14a**, **1** and CS055 for 48h, and measured by flow cytometry with FITC-Annexin V/PI staining. Data are expressed as means ± SD of the percentages of apoptotic cells from three independent experiments.

2.2.7. Determination of immunofluorescence and ROS generation

Since the docking results revealed a potent affinity between CDK2 and HDAC1 with the representative compounds, we assessed the effects of **7c** and **14a** on the inhibition of CDK2 and the deacetylation of histone H3. Compounds showed favorable antiproliferative activity for A375 cells which possessed a good cell adhesion property, so A375 cell line was selected as the model. The immunofluorometric analysis was illustrated in **Figure 8A** and **8B**. It's demonstrated that **7c** and **14a** could lead to an apparent inhibition of CDK2 compared to control (DMSO) (**Fig. 8A**). They also induced an increase of acetylation of H3K9(**Fig. 8B**), which suggested that **7c** and **14a** might alter the acetylation of H3, inhibiting HDAC activity. These findings elucidated that compounds **7c** and **14a** acted as efficient CDK2 and HDAC inhibitors.

Reactive oxygen species (ROS) play a critical role in cellular processes involving cell growth, proliferation, development, differentiation, senescence and apoptosis[61, 62]. High levels of intracellular ROS might cause DNA damage, and ultimately resulted in cell death. The 2,7-dichlorofluorescein diacetate (DCFH-DA) is frequently applied for intracellular ROS detection. As mentioned in **Figure 8C**, the green fluorescence signal was hardly observed in the control group. In contrast, after treatment with the compounds **7c** and **14a**, cells displayed strong green fluorescence, indicating a significant increase in intracellular ROS levels. Accordingly, compounds **7c** and **14a** might accelerate intracellular ROS accumulation, leading to cancer cell death.

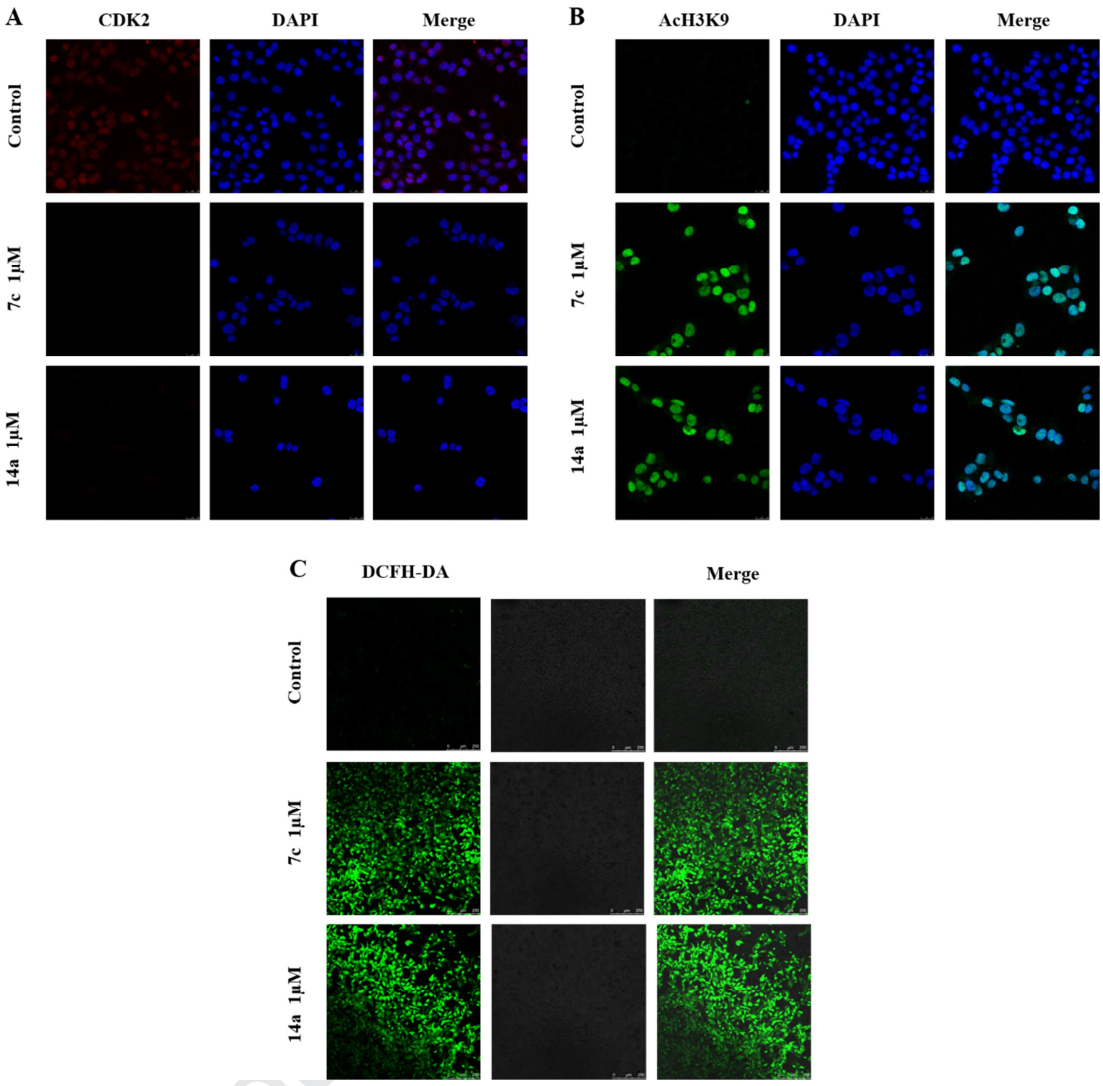

Figure 8. A375 cells were treated with **7c** and **14a** at 1μM or DMSO for 12h. Immunofluorescence images of (A) CDK2, DAPI and (B) AcH3K9, DAPI staining and merge in untreated or treated cells. (C) A375 cells were treated with **7c** and **14a** at 1μM or DMSO for 24h.Fluorescence images of intracellular ROS generation.

2.2.8 Pharmacokinetic parameters

Considering that compounds **7c** and **14a** exhibited excellent *in vitro* antitumor activity, the pharmacokinetic properties (PK) were investigated in ICR male mice. Compounds **7c** and **14a** were administered intraperitoneally (IP) at a dose of 20mg/kg respectively. The PK parameters were presented **Table 4**. The half-life ($t_{1/2}$) of compound **7c** was 2.61h, the maximum plasma concentration (C_{max}) was 7570 ng/mL, and the area under concentration-time curve ($AUC_{0-\infty}$) was 30700 ng h/mL. However, compound **14a** showed a short half-life of 1.63h, a C_{max} of 2170 ng/mL and an $AUC_{0-\infty}$ of 7200 ng h/mL. In addition, compared with **14a** (F=27.8%), compound **7c** showed higher bioavailability with F= 63.6%. The data indicated that compound **7c** possessed better pharmacokinetic properties than **14a**.

Table 5

Pharmacokinetic parameters of **7c** and **14a** in ICR mice

Compd	**7c**	**14a**
Dose (mg/kg)	20	20
administration	i.p.	i.p.
$t_{½}$ (h)	2.61	1.63
T_{max} (h)	2.00	1.00
C_{max} (ng/mL)	7570	2170
$AUC_{0-\infty}$ (ng h/mL)	30700	7200
$MRT_{0-\infty}$ (ng h/mL)	3.31	2.36
F (%)	63.6	27.8

2.2.9 *In vivo* antitumor activity of compound **7c**

As compound **7c** exhibited excellent antiproliferative activity towards HCT116 cells (IC_{50}= 0.71μM) over other cell lines, we decided to evaluate the *in vivo* antitumor efficacy of compound **7c** in the HCT116 xenograft nude mice models. When tumors grew to a volume of 100-300 mm^3, the BALB/c female mice were randomly divided into treatment and control groups (6 mice per group). Compound **7c** was intraperitoneally administered at 25 and 12.5 mg/kg once daily (QD) for 21 days. No significant body weight changes and toxicity signs were observed in the treatment groups (**Fig. 9A**). Compound **7c** effectively inhibited the growth of HCT116 xenograft tumors compared to control. The tumor growth inhibitions (TGI) of **7c** at 12.5 and 25 mg/kg were 37.0% and 51.0% respectively (**Fig.9B-D**). These results demonstrated that compound **7c** possessed remarkable in vivo antitumor efficacy.

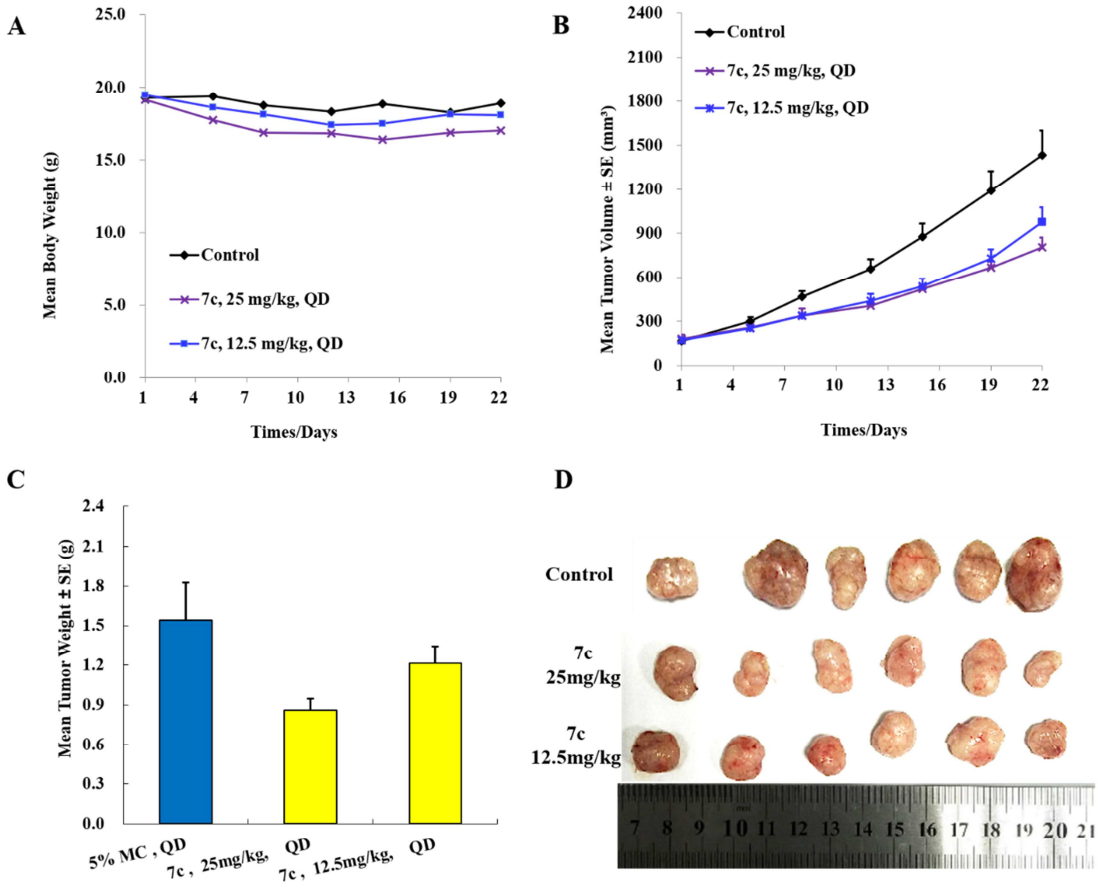

Figure 9. *In vivo* antitumor potency of compound **7c** against HCT116 xenografts models with intraperitoneal administration. (A) Body weight and (B) tumor volume measurements for **7c** treated mice groups after 21 days. (C) Comparison of the final tumor weights in each group after the 21 days treatment period of **7c**. (D) The picture of dissected HCT116 tumor tissues.

3. Conclusions

In summary, we have successfully designed and synthesized novel dual HDAC/CDK inhibitors. The representative compounds (**7c** and **14a)** displayed potent antiproliferative activities against five selected human cancer cell lines with IC_{50} values ranging from 0.71 to 7.76μM. The compounds **7c** and **14a** also showed excellent HDAC and CDK inhibition with IC_{50} values at the nanomolar level. Moreover, compounds **7c** and **14a** significantly arrested cell cycle at G2/M phase and promoted apoptosis towards A375 cell line, HCT116 cell line, H460 cell line and Hela cell line. In addition, the immunofluorometric analysis indicated that **7c** and **14a** displayed significant inhibition of CDK2 and an increase of the acetylation of H3K9. They could also enhance ROS levels, and then cause cell death. Furthermore, the *in vivo* studies indicated that compound **7c** showed good pharmacokinetic profile, and also exhibited potent antitumor efficacy in the HCT116 xenograft model (TGI= 51.0%).

4. Experimental section

4.1 Chemistry

^{1}H NMR and ^{13}C NMR spectra were recorded on a Bruker AV III 400 spectrometer (400MHz) using DMSO-d_6 as solvent. The chemical shifts were measured in parts per million (ppm) relative to Me_4Si as internal standard. High-resolution mass spectra (HRMS) were obtained on an Agilent Q-TOF 6540 mass spectrometer. All reagents and solvents were purchased from commercial sources and were used without further purification. The progress of all reactions was monitored by thin layer chromatography (TLC), and precoated plates with silica gel F254 were purchased from Qingdao Haiyang Chemical Co. Ltd. All the final compounds were obtained ≥ 90% purity, as tested by high-performance liquid chromatography (HPLC) on a Thermo Scientific ™ UltiMate ™ 3000 systerm (column, C18, 5mm, 4.6mm × 250mm; mobile phase, gradient elution of methanol/ H_2O (0.1% H_3PO_4); flow rate, 1.0mL/min; temperature, 35°C). Analyses indicated by the symbols of the elements or functions were within 0.4% of the theoretical values.

4.1.1. methyl 4-((4-nitro-1H-pyrazole-3-carboxamido)methyl)benzoate (**4**) Yield: 65%; 4-nitro-1H-pyrazole-3-carboxylic acid (3.18mmol, 1.1equiv), methyl 4-(aminomethyl)benzoate hydrochloride (2.89mmol, 1equiv), EDCI (3.47mmol, 1.2equiv), HOBt (3.47mmol, 1.2equiv), DIEA (6.94mmol, 2.4equiv) were mixed in DMF (20mL). The reaction was stirred for 12h at room temperature. TLC analysis, using petroleum ether: ethyl acetate (1:2) as the eluent, indicated the complete reaction. The mixture was diluted with a large amount of water and then extracted with ethyl acetate. The organic layer was collected and dried by anhydrous sodium sulfate. The solvent was concentrated to obtain **4** as a light purple solid. ^{1}H NMR (400MHz, DMSO-d_6): δ=7.91(3H, m), 7.50(2H, m), 4.50(2H, s), 3.84(3H, s); HRMS (ESI) $(M+H)^+$ Calc'd for $C_{13}H_{12}N_4O_5$: 305.0887 Found:305.0884.

4.1.2. methyl 4-((4-amino-1H-pyrazole-3-carboxamido)methyl)benzoate (**5**) Yield: 93%; To a 100mL, one-necked flask, sequentially charged with compound **4** (1.64mmol, 1equiv), $HCOONH_4$ (8.20mmol, 5equiv) in 16mL of the mixed solvent of tetrahydrofuran and isopropanol (1:1). While stirring vigorously under nitrogen, palladium 5% on activated carbon (182mg, wetted with ca. 55% Water) was added into the mixture. The reaction was heated at reflux for 1h. When TLC analysis showed the complete reaction, the mixture was cooled to ambient temperature, and isolated by filtration. Then the filtrate was concentrated in vacuo to afford **5** as a solid. ^{1}H NMR (400MHz, DMSO-d_6): δ=7.91(2H, d, *J*=8.12Hz), 7.44(2H, m), 7.10(2H, s), 4.60(2H, s), 4.47(2H, m), 3.84(3H, s); HRMS (ESI) $(M+H)^+$ Calc'd for $C_{13}H_{14}N_4O_3$: 275.1145 Found:275.1141.

4.1.3. methyl 4-((4-(2,6-dichlorobenzamido)-1H-pyrazole-3-carboxamido)methyl)benzoate (**6c**)

Yield: 87%; A mixture of compound **5** (1.82mmol, 1equiv), triethylamine (2.18mmol, 1.2equiv) was stirred in 20mL of 1,4-dioxane. Then 2,6-dichlorobenzoyl chloride (2.00mmol, 1.1equiv) was added dropwise into the solution in an ice bath. The reaction was stirred for 12h at 0□. TLC analysis (petroleum ether: ethyl acetate=1:1) indicated the complete reaction. The mixture was filtered, and then the filtrate was evaporated under reduced pressure. The crude product was further purified by flash column chromatography with an appropriate ethyl acetate/petroleum ether mixture to provide the product **6c**. ^{1}H NMR (400MHz, DMSO-d_6): δ=13.48(1H, s), 10.09(1H, s), 9.15(1H, s), 8.37(1H, s), 7.91 (2H, d, *J*=8.34Hz), 7.36 (5H, m),4.48 (2H, d, *J*=6.66Hz), 3.83(3H, s); HRMS (ESI) $(M+H)^+$ Calc'd for $C_{20}H_{16}Cl_2N_4O_4$: 447.0628 Found:447.0619.

Compounds **6a-6b** and **6e-6g** were prepared according to a similar procedure described for **6c**.

General Procedure for the synthesis of compounds **7a-7g**. Compound **6** (1.32mmol, 1equiv) was dissolved in 20mL of 1,4-dioxane. Then aqueous sodium hydroxide solution (2mol/L, 5equiv) was added into this mixture. The reaction was heated for 1h at 85□. When TLC analysis indicated the complete reaction, the reaction mixture was cooled to ambient temperature, concentrated in vacuo, and acidified with 2N HCl (pH at 5-6) to form precipitation. The precipitate was isolated by filtration and dried to afford the corresponding acid as a white solid. Subsequently, 2-(1H-Benzotriazole-1-yl)-1,1,3,3-tetramethyluronium hexafluorophosphate (HBTU, 1.77mmol, 1.5equiv), the aforementioned acid (1.18mmol, 1equiv) and trimethylamine (1.77mmol, 1.5equiv) were dissolved in DMF (15mL). The mixture was stirred at room temperature for 10min. Afterwards benzene-1,2-diamine (1.18mmol, 1equiv) was added into the solution for another 3h. When TLC analysis (petroleum ether: ethyl acetate=1:3) indicated the complete reaction, the reaction mixture was diluted with water, and extracted with ethyl acetate. Then the organic layer was dried by anhydrous Na_2SO_4 and concentrated in vacuo. The crude product was further purified by flash column chromatography with an appropriate ethyl acetate/petroleum ether mixture to provide the target compounds **7a-7g**.

4.1.4.

N-(4-((2-aminophenyl)carbamoyl)benzyl)-4-(2,6-difluorobenzamido)-1H-pyrazole-3-carboxamide (**7a**) Yield: 75%; HPLC Rt= 3.002min; ^{1}H NMR (400MHz, DMSO-d_6): δ= 9.65(1H, s), 9.21(1H, s), 8.37(1H, s), 7.93(2H, m), 7.61(1H, m), 7.42(2H, m), 7.25(2H, m), 7.17(1H, d, *J*=7.16Hz), 6.97(1H, m), 6.80(1H, m), 6.60(1H, t, *J*=7.59Hz), 4.90(2H, s), 4.51(2H, s); ^{13}C NMR (400MHz, DMSO-d_6): δ= 163.86, 160.94, 158.45, 156.70, 143.56, 140.86, 133.70, 133.36, 128.39, 128.30, 128.02, 127.81, 127.70, 127.47, 124.91, 122.07, 121.33, 116.58, 112.98, 112.75, 42.13ppm. HRMS (ESI) $(M+H)^+$ Calc'd for $C_{25}H_{20}F_2N_6O_3$: 491.1644 Found:491.1637.

4.1.5.

N-(4-((2-aminophenyl)carbamoyl)benzyl)-4-(2-chloro-6-fluorobenzamido)-1H-pyrazole-3-carboxamide (**7b**) Yield: 63%; HPLC Rt= 2.992min; ^{1}H NMR (400MHz, DMSO-d_6): δ= 13.47(1H, s), 10.23(1H, s), 9.62(1H, s), 8.40(1H, s), 7.92(3H, m), 7.43(5H, m), 7.16(1H, d, *J*=7.04Hz), 6.97(1H, m), 6.79(1H, m), 6.60(1H, t, *J*=7.73Hz), 4.93(2H, s), 4.49(2H, d, *J*=6.00Hz); ^{13}C NMR (400MHz, DMSO-d_6): δ= 163.32, 160.12, 158.33, 157.65, 143.07, 133.12, 132.30, 132.21, 131.13, 131.08, 127.82, 127.77, 126.99, 126.63, 126.42, 125.75, 123.28, 121.44, 120.91, 116.21, 116.07, 115.07, 114.86, 41.57ppm. HRMS (ESI) $(M+H)^+$ Calc'd for $C_{25}H_{20}ClFN_6O_3$: 507.1348 Found:507.1340.

4.1.6.

N-(4-((2-aminophenyl)carbamoyl)benzyl)-4-(2,6-dichlorobenzamido)-1H-pyrazole-3-carboxamide (**7c**) Yield: 45%; HPLC Rt= 2.975min; ^{1}H NMR (400MHz, DMSO-d_6): δ= 13.45(1H, s), 10.11(1H, s), 9.59(1H, s), 9.15(1H, m), 8.38(1H, s), 7.92(2H, m), 7.56(3H, m), 7.42(2H, m), 7.15(1H, d, *J*=8.10Hz), 6.96(1H, m), 6.78(1H, m), 6.59(1H, t, *J*=7.70Hz), 4.87(2H, s), 4.48(2H, d, *J*=5.71Hz); ^{13}C NMR (400MHz, DMSO-d_6): δ= 163.83, 160.88, 143.56, 135.85, 133.62, 133.30, 132.31, 131.72, 128.86, 128.26, 127.50, 127.11, 126.90, 123.78, 121.92, 121.35, 116.70, 116.56, 42.07ppm. HRMS (ESI) $(M+H)^+$ Calc'd for $C_{25}H_{20}Cl_2N_6O_3$: 523.1053 Found: 523.1049.

4.1.7.

N-(4-((2-aminophenyl)carbamoyl)benzyl)-4-benzamido-1H-pyrazole-3-carboxamide (**7d**) Yield: 68%; HPLC Rt= 2.962min; ^{1}H NMR (400MHz, DMSO-d_6): δ= 13.41(1H, s), 10.70(1H, s), 9.70(1H, s), 9.23(1H, s), 8.37(1H, s), 7.89(4H, m), 7.60(4H, m), 7.49(2H, m), 7.19(1H, d, *J*=7.84Hz), 7.02(1H, m), 7.83(1H, d, *J*=7.56Hz), 6.66(1H, m), 4.58(2H, m), 2.69(2H, m); ^{13}C NMR (400MHz, DMSO-d_6): δ= 165.67, 164.49, 163.13, 143.54, 142.52, 133.73, 133.54, 133.06, 132.49, 129.50, 128.32, 127.45, 127.17, 126.96, 124.33, 123.23, 120.61, 117.53, 117.11, 42.05, 38.70ppm. HRMS (ESI) $(M+H)^+$ Calc'd for $C_{25}H_{22}N_6O_3$: 455.1832 Found: 455.1825.

4.1.8.

N-(4-((2-aminophenyl)carbamoyl)benzyl)-4-(2-chlorobenzamido)-1H-pyrazole-3-carboxamide (**7e**) Yield: 60%; HPLC Rt= 2.948min; ^{1}H NMR (400MHz, DMSO-d_6): δ= 10.25(1H, s), 9.46(1H, s), 9.19(1H, s), 8.37(1H, s), 7.94(2H, m), 7.72(1H, m), 7.44(6H, m), 7.17(1H, m), 6.97(1H, t, *J*=7.59Hz), 6.78(1H, d, *J*=7.68Hz), 6.60(1H, t, *J*=8.24Hz), 4.89(2H, s), 4.50(2H, s); ^{13}C NMR (400MHz, DMSO-d_6): δ= 165.61, 164.00, 162.92, 143.57, 135.31, 133.61, 132.48, 130.70, 130.38, 130.05, 128.27, 128.14, 127.48, 127.13, 126.91, 123.79, 122.59, 116.72, 116.58, 42.03ppm. HRMS (ESI) $(M+H)^+$ Calc'd for $C_{25}H_{21}ClN_6O_3$: 489.1443 Found: 489.1445.

4.1.9.

N-(4-((2-aminophenyl)carbamoyl)benzyl)-4-(2-fluorobenzamido)-1H-pyrazole-3-carboxamide (**7f**) Yield: 67%; HPLC Rt= 2.945min; ^{1}H NMR (400MHz, DMSO-d_6): δ= 13.40(1H, s), 10.88(1H, m), 9.71(1H, s), 9.15(1H, m), 8.41(1H, s), 8.03(1H, m),

7.97(2H, m), 7.66(1H, m), 7.48(2H, m), 7.41(2H, m), 7.20(1H, d, *J*=7.52Hz), 7.01(1H, m), 6.85(1H, d, *J*=7.88Hz), 6.69(1H, m), 4.56(2H, d, *J*=6.07Hz); ^{13}C NMR (400MHz, DMSO-d_6): δ= 165.21, 163.59, 161.02, 159.00, 158.55, 134.18, 132.98, 131.28, 127.82, 126.99, 126.65, 126.47, 125.22, 124.12, 122.24, 120.70, 120.48, 120.36, 117.45, 116.89, 116.63, 116.40, 41.52, 38.21ppm. HRMS (ESI) $(M+H)^+$ Calc'd for $C_{25}H_{21}FN_6O_3$: 473.1738 Found: 473.1740.

4.1.10.
N-(4-((2-aminophenyl)carbamoyl)benzyl)-4-(2-methoxybenzamido)-1H-pyrazole-3-carboxamide (**7g**) Yield: 80%; HPLC Rt= 2.967min; ^{1}H NMR (400MHz, DMSO-d^6): δ= 11.76(1H, s), 9.66(1H, s), 9.06(1H, s), 8.41(1H, s), 8.12(1H, m), 7.96(2H, m), 7.57(1H, m), 7.48(2H, m), 7.24(2H, m), 7.12(2H, m), 7.02(1H, m), 6.80(1H, m), 6.60(1H, m), 4.90(2H, s), 4.59(2H, d, *J*=5.98Hz), 4.07(3H, s); ^{13}C NMR (400MHz, DMSO-d^6): δ= 163.29, 160.93, 157.44, 143.25, 143.06, 141.17, 133.53, 133.10, 131.35, 127.77, 127.14, 126.62, 126.36, 124.59, 123.33, 122.51, 120.84, 120.16, 117.60, 116.22, 116.09, 114.42, 112.28, 55.91, 41.54ppm. HRMS (ESI) $(M+H)^+$ Calc'd for $C_{26}H_{24}N_6O_4$: 485.1938 Found:485.1929.

General Procedure for the synthesis of **8a-8g**. A solution of KOH (2.84g, 50.6mmol) in MeOH (7mL) was added dropwise into a solution of hydroxylamine hydrochloride (2.34g, 33.7mmol) in MeOH (12mL) in an ice bath. The mixture was stirred at 0□ for 1h, and then was filtered to obtain a fresh solution of NH_2OH in MeOH. Then compound **6** (0.22mmol, 1equiv) was dissolved in 3mL of the aforementioned fresh solution of NH_2OH. The mixture was stirred for 1h at room temperature. TLC analysis (ethyl acetate: methanol=5:1) indicated the complete reaction. The reaction mixture was evaporated under reduced pressure, and was acidified with 2N HCl (pH at 5-6) to form precipitation. The precipitate was isolated by filtration and dried to afford the corresponding compounds **8a-8g** as a white solid.

4.1.11.
4-(2,6-difluorobenzamido)-N-(4-(hydroxycarbamoyl)benzyl)-1H-pyrazole-3-carboxamide (**8a**) Yield: 89%; HPLC Rt= 2.993min; ^{1}H NMR (400MHz, DMSO-d_6): δ= 13.46(1H, s), 11.14(1H, s), 10.26(2H, s), 9.08(1H, s), 8.29(1H, s), 7.65(3H, m), 7.30(2H, m), 7.18(2H, m), 4.40(2H, m); ^{13}C NMR (400MHz, DMSO-d_6): δ= 164.09, 163.31, 160.44, 157.95, 156.22, 142.68, 132.86, 131.23, 129.34, 127.04, 126.87, 121.59, 113.62, 112.49, 112.24, 41.48ppm. HRMS (ESI) $(M+H)^+$ Calc'd for $C_{19}H_{15}F_2N_5O_4$: 416.1171 Found: 416.1168.

4.1.12.
4-(2-chloro-6-fluorobenzamido)-N-(4-(hydroxycarbamoyl)benzyl)-1H-pyrazole-3-carboxamide (**8b**) Yield: 81%; HPLC Rt= 2.975min; ^{1}H NMR (400MHz, DMSO-d_6): δ= 13.45(1H, s), 11.16(1H, s), 10.20(1H, s), 9.12(1H, s), 9.00(1H, s), 8.38(1H, s), 7.69(2H, d, *J*=8.45Hz), 7.55(1H, m), 7.37(4H, m), 4.46(2H, m); ^{13}C NMR (400MHz, DMSO-d_6): δ= 164.57, 163.78, 160.61, 158.84, 158.14, 143.16, 132.79, 132.70, 131.76, 129.83, 127.55, 127.35, 126.24, 121.92, 121.40, 115.56, 115.34, 42.00ppm.

HRMS (ESI) $(M+H)^+$ Calc'd for $C_{19}H_{15}ClFN_5O_4$: 432.0876 Found: 432.0872.

4.1.13.
4-(2,6-dichlorobenzamido)-N-(4-(hydroxycarbamoyl)benzyl)-1H-pyrazole-3-carboxamide (**8c**) Yield: 73%; HPLC Rt= 2.970min; ^{1}H NMR (400MHz, DMSO-d_6): δ= 10.13(1H, s), 9.17(1H, s), 8.39(1H, s), 7.71(2H, d, *J*=8.40Hz), 7.56(4H, m), 7.38(2H, m), 4.47(2H, m); ^{13}C NMR (400MHz, DMSO-d_6): δ= 164.04, 163.20, 160.45, 142.64, 135.33, 131.80, 131.23, 129.30, 128.34, 127.08, 126.88, 121.43, 41.51ppm. HRMS (ESI) $(M+H)^+$ Calc'd for $C_{19}H_{15}Cl_2N_5O_4$: 448.0580 Found: 448.0576.

4.1.14. 4-benzamido-N-(4-(hydroxycarbamoyl)benzyl)-1H-pyrazole-3-carboxamide (**8d**) Yield: 82%; HPLC Rt= 2.945min; ^{1}H NMR (400MHz, DMSO-d_6): δ= 13.50(1H, s), 11.24(1H, s), 10.69(1H, s), 9.22(1H, s), 8.36(1H, s), 7.88(2H, d, *J*=7.48Hz), 7.74(2H, d, *J*=8.04Hz), 7.58(4H, m), 7.42(2H, d, *J*=7.94Hz), 4.55(2H, d, *J*=5.78Hz); ^{13}C NMR (400MHz, DMSO-d_6): δ= 164.09, 162.65, 142.68, 133.23, 131.98, 131.27, 129.38, 128.99, 127.16, 127.02, 126.91, 126.68, 122.75, 41.48ppm. HRMS (ESI) $(M+H)^+$ Calc'd for $C_{19}H_{17}N_5O_4$: 380.1360 Found: 380.1358.

4.1.15.
4-(2-chlorobenzamido)-N-(4-(hydroxycarbamoyl)benzyl)-1H-pyrazole-3-carboxamide (**8e**) Yield: 76%; HPLC Rt= 2.948min; ^{1}H NMR (400MHz, DMSO-d_6): δ= 13.44(1H, s), 11.17(1H, s), 10.22(1H, s), 9.12(1H, m), 8.99(1H, s), 8.36(1H, s), 7.71(3H, m), 7.58(2H, m), 7.48(1H, m), 7.36(2H, d, *J*=7.80Hz), 4.47(2H, d, *J*=6.39Hz); ^{13}C NMR (400MHz, DMSO-d_6): δ= 164.56, 164.04, 162.89, 143.17, 135.27, 133.13, 132.49, 131.76, 130.70, 130.37, 130.04, 129.84, 128.13, 127.55, 127.37, 122.52, 120.94, 41.94ppm. HRMS (ESI) $(M+H)^+$ Calc'd for $C_{19}H_{16}ClN_5O_4$: 414.0970 Found:414.0958.

4.1.16.
4-(2-fluorobenzamido)-N-(4-(hydroxycarbamoyl)benzyl)-1H-pyrazole-3-carboxamide (**8f**) Yield: 82%; HPLC Rt= 2.972min; ^{1}H NMR (400MHz, DMSO-d_6): δ= 13.50(1H, s), 11.24(1H, s), 10.87(1H, d, *J*=10.59Hz), 9.16(1H, s), 8.41(1H, s), 8.04(1H, t, *J*=7.65Hz), 7.74(4H, m), 7.42(4H, m), 4.53(2H, d, *J*=6.22Hz); ^{13}C NMR (400MHz, DMSO-d_6): δ= 161.01, 159.01, 158.54, 142.76, 134.25, 134.16, 131.26, 129.36, 127.17, 127.05, 126.90, 125.20, 125.17, 122.27, 120.49, 120.37, 116.62, 116.38, 41.44ppm. HRMS (ESI) $(M+H)^+$ Calc'd for $C_{19}H_{16}FN_5O_4$: 398.1265 Found:398.1256.

4.1.17.
N-(4-(hydroxycarbamoyl)benzyl)-4-(2-methoxybenzamido)-1H-pyrazole-3-carboxamide (**8g**) Yield: 88%; HPLC Rt= 2.978min; ^{1}H NMR (400MHz, DMSO-d_6): δ= 11.74(1H, s), 11.21(1H, s), 9.00(1H, m), 8.39(1H, s), 8.10(1H, m), 7.72(2H, m), 7.55(1H, m), 7.43(2H, m), 7.21(1H, d, *J*=8.59Hz), 7.11(1H, t, *J*=7.62Hz), 4.54(2H, d, *J*=6.16Hz), 4.05(3H, s); ^{13}C NMR (400MHz, DMSO-d_6): δ= 164.57, 163.76, 161.45,

157.92, 143.45, 134.04, 131.84, 131.72, 127.71, 127.38, 122.98, 121.33, 120.61, 112.77, 56.39, 41.95ppm. HRMS (ESI) $(M+H)^+$ Calc'd for $C_{20}H_{19}N_5O_5$: 410.1465 Found:410.1463.

4.1.18. methyl 4-amino-1H-pyrazole-3-carboxylate (**10**) Yield: 88%; Methyl 4-nitro-1H-pyrazole-3-carboxylate (2.92mmol, 1equiv), $HCOONH_4$ (14.6mmol, 5equiv) was dissolved in 16mL of the mixed solvent of tetrahydrofuran and isopropanol (1:1). While stirring vigorously under nitrogen, palladium 5% on activated carbon (182mg, wetted with ca. 55% Water) was added into the mixture. The reaction was heated at reflux for 1h. Upon cooling to ambient temperature, the mixture was filtered. The filtrate was evaporated under reduced pressure to afford compound **10** as a solid. ^{1}H NMR (400MHz, DMSO-d_6): δ=12.82(1H, s), 7.09(1H, s), 4.86(2H, s), 3.77(3H, s); HRMS (ESI) $(M+H)^+$ Calc'd for $C_5H_7N_3O_2$: 142.0617 Found:142.0612.

4.1.19. 4-(2,6-dichlorobenzamido)-1H-pyrazole-3-carboxylic acid (**12a**) Yield: 73%; A mixture of compound **10** (3.54mmol, 1equiv), triethylamine (4.25mmol, 1.2equiv) was stirred in 20mL of 1,4-dioxane. Then 2,6-dichlorobenzoyl chloride (3.89mmol, 1.1equiv) was added dropwise into the solution in an ice bath. The reaction was stirred for 12h at 0□. TLC analysis (petroleum ether: ethyl acetate=1:1) indicated the complete reaction. The mixture was filtered to obtain the crude product **11a** in 1,4-dioxane. Then the filtrate was used in the next step without further isolation. An aqueous sodium hydroxide solution (2mol/L, 5equiv) was added into the above filtrate. The reaction was heated at 85□ for 1h. When TLC analysis indicated the complete reaction, the reaction mixture was cooled to ambient temperature, concentrated in vacuo, and acidified with 2N HCl (pH at 5-6) to form precipitation. The precipitate was isolated by filtration and dried to afford the corresponding acid **12a** as a white solid. ^{1}H NMR (400MHz, DMSO-d_6): δ=13.44(1H, s), 9.87(1H, s), 8.29(1H, s), 7.55 (3H, m); HRMS (ESI) $(M+H)^+$ Calc'd for $C_{11}H_7Cl_2N_3O_3$: 299.9943 Found:299.9929.

Compounds **12b-12g** were prepared according to a similar procedure described for **12a**.

4.1.20. ethyl 2-(4-(4-(2,6-dichlorobenzamido)-1H-pyrazole-3-carboxamido)phenyl)acetate (**13a**) Yield: 69%; **12a** (2.16mmol, 1equiv), ethyl 2-(4-aminophenyl)acetate (2.16mmol, 1equiv), EDCI (2.59mmol, 1.2equiv), HOBt (2.59mmol, 1.2equiv) and DIEA (2.59mmol, 1.2equiv) were mixed in DMF (20mL). TLC analysis, using petroleum ether: ethyl acetate (1:2) as the eluent, indicated the complete reaction. The mixture was diluted with water and then extracted with ethyl acetate. The organic layer was collected and dried by anhydrous sodium sulfate. The solvent was concentrated to provide compound **13a** as a solid. ^{1}H NMR (400MHz, DMSO-d_6): δ=10.31(1H, s), 10.15(1H, s), 8.44(1H, s), 7.68 (2H, m), 7.58 (4H, m), 7.21 (2H, d, *J*=8.46Hz), 4.09 (2H, m), 3.61(2H, s), 1.24(3H, m); HRMS (ESI) $(M+H)^+$ Calc'd for $C_{21}H_{18}Cl_2N_4O_4$:

461.0784 Found:461.0784.

Compounds **13b-13g** were prepared according to a similar procedure described for **13a**.

General Procedure for the synthesis of **14a-14g**. Compound **13** (1.32mmol, 1equiv) was dissolved in 20mL of 1,4-dioxane. Then aqueous sodium hydroxide solution (2mol/L, 5equiv) was added into this mixture. The reaction was heated at 85□ for 1h. When TLC analysis indicated the complete reaction, the reaction mixture was cooled to ambient temperature, concentrated in vacuo, and acidified with 2N HCl (pH at 5-6) to form precipitation. The precipitate was isolated by filtration and dried to afford the corresponding acid as a white solid. Subsequently, HBTU (1.77mmol, 1.5equiv), the aforementioned acid (1.18mmol, 1equiv) and trimethylamine (1.77mmol, 1.5equiv) was dissolved in DMF (15 mL). The mixture was stirred at room temperature for 10min. Afterwards benzene-1,2-diamine (1.18mmol, 1equiv) was added into the solution for another 5h. When TLC analysis (petroleum ether: ethyl acetate=1:3) indicated the complete reaction, the mixture was diluted with water, and extracted with ethyl acetate. Then the organic layer was dried by anhydrous Na_2SO_4 and was concentrated in vacuo. The crude product was further purified by flash column chromatography with an appropriate ethyl acetate/petroleum ether mixture to provide the target compounds **14a-14g**.

4.1.21.
N-(4-(2-((2-aminophenyl)amino)-2-oxoethyl)phenyl)-4-(2,6-dichlorobenzamido)-1H-pyrazole-3-carboxamide (**14a**) Yield: 43%; HPLC Rt= 2.983min; ^{1}H NMR (400MHz, DMSO-d_6): δ= 13.60(1H, s), 10.33(1H, s), 10.17(1H, s), 9.37(1H, s), 8.46(1H, s), 7.75(2H, d, *J*=8.18Hz), 7.57(2H, m), 7.52(1H, m), 7.30(2H, d, *J*=8.46Hz), 7.16(1H, m), 6.90(1H, m), 6.73(1H, m), 6.54(1H, m), 3.62(2H, s), 2.69(2H, s); ^{13}C NMR (400MHz, DMSO-d_6): δ= 169.18, 161.74, 160.65, 141.78, 136.58, 135.47, 133.31, 131.73, 131.30, 129.13, 128.31, 125.88, 125.29, 123.34, 121.68, 121.39, 120.57, 116.25, 115.90, 42.12, 38.21ppm. HRMS (ESI) $(M+H)^+$ Calc'd for $C_{25}H_{20}Cl_2N_6O_3$: 523.1053 Found: 523.1051.

4.1.22.
N-(4-(2-((2-aminophenyl)amino)-2-oxoethyl)phenyl)-4-(2-chloro-6-fluorobenzamido)-1H-pyrazole-3-carboxamide (**14b**) Yield: 53%; HPLC Rt= 2.962min;
^{1}H NMR (400MHz, DMSO-d_6): δ= 13.59(1H, s), 10.73(1H, d, *J*=6.67Hz), 10.32(1H, s), 10.25(1H, s), 9.35(1H, m), 8.45(1H, s), 7.74(2H, t, *J*=8.92Hz), 7.56(1H, m), 7.46(1H, m), 7.38(2H, m), 7.31(1H, m), 7.16(1H, m), 6.90(1H, m), 6.73(1H, m), 6.53(1H, m), 3.61(2H, m), 3.03(2H, s); ^{13}C NMR (400MHz, DMSO-d_6): δ= 169.17, 161.71, 160.19, 158.58, 157.72, 141.74, 136.59, 133.32, 132.23, 131.74, 131.18, 129.13, 125.87, 125.70, 125.29, 123.36, 121.66, 120.55, 116.28, 115.91, 115.03, 114.81, 42.12, 38.21ppm. HRMS (ESI) $(M+H)^+$ Calc'd for $C_{25}H_{20}ClFN_6O_3$: 507.1348 Found: 507.1342.

4.1.23.

N-(4-(2-((2-aminophenyl)amino)-2-oxoethyl)phenyl)-4-(2,6-difluorobenzamido)-1H-pyrazole-3-carboxamide (**14c**) Yield: 61%; HPLC Rt= 2.972min; ^{1}H NMR (400MHz, DMSO-d_6): δ= 10.34(1H, s), 9.38(1H, s), 8.43(1H, s), 7.76 (2H, d, *J*=8.36Hz), 7.63(1H, m), 7.27(5H, m), 7.17(1H, m), 6.90(1H, m), 6.73(1H, m), 6.54(1H, m), 4.84(2H, s), 3.62(2H, s); ^{13}C NMR (400MHz, DMSO-d_6): δ= 169.17, 161.71, 160.51, 160.44, 158.02,, 157.95, 156.48, 141.92, 136.61, 131.76, 129.15, 125.86, 125.29, 123.28, 120.54, 116.14, 115.82, 112.46, 112.22, 42.13ppm. HRMS (ESI) $(M+H)^+$ Calc'd for $C_{25}H_{20}F_2N_6O_3$: 491.1644 Found: 491.1645.

4.1.24.

N-(4-(2-((2-aminophenyl)amino)-2-oxoethyl)phenyl)-4-benzamido-1H-pyrazole-3-carboxamide (**14d**) Yield: 66%; HPLC Rt= 2.963min; ^{1}H NMR (400MHz, DMSO-d_6): δ= 13.52(1H, s), 10.59(1H, s), 10.37(1H, m), 8.42(1H, s), 7.91(6H, m), 7.62(5H, m), 7.35(2H, m), 3.64(4H, m); ^{13}C NMR (400MHz, DMSO-d_6): δ= 163.27, 162.98, 133.76, 133.40, 132.53, 129.67, 129.52, 127.24, 123.57, 121.37, 121.04, 116.69, 116.36ppm. HRMS (ESI) $(M+H)^+$ Calc'd for $C_{25}H_{22}N_6O_3$: 455.1832 Found: 455.1826.

4.1.25.

N-(4-(2-((2-aminophenyl)amino)-2-oxoethyl)phenyl)-4-(2-chlorobenzamido)-1H-pyrazole-3-carboxamide (**14e**) Yield: 67%; HPLC Rt= 2.965min; ^{1}H NMR (400MHz, DMSO-d_6): δ= 9.38(1H, s), 8.39(1H, s), 7.74(3H, m), 7.59(4H, m), 7.30(2H, d, *J*=8.11Hz), 7.16(1H, m), 6.89(1H, m), 6.73(1H, m), 6.53(1H, m), 4.83(2H, s), 3.61(2H, s); ^{13}C NMR (400MHz, DMSO-d_6): δ= 169.18, 162.63, 161.97, 141.91, 136.65, 131.87, 131.69, 130.18, 129.92, 129.63, 129.15, 127.60, 125.84, 125.27, 123.29, 120.52, 116.13, 115.81, 42.13ppm. HRMS (ESI) $(M+H)^+$ Calc'd for $C_{25}H_{21}ClN_6O_3$: 489.1443 Found: 489.1444.

4.1.27.

N-(4-(2-((2-aminophenyl)amino)-2-oxoethyl)phenyl)-4-(2-fluorobenzamido)-1H-pyrazole-3-carboxamide (**14f**) Yield: 70%; HPLC Rt= 2.953min; ^{1}H NMR (400MHz, DMSO-d_6): δ= 10.82(1H, m), 10.36(1H, s), 9.53(1H, m), 8.46(1H, s), 8.05(1H, m), 7.80(2H, m), 7.68(1H, m), 7.42(4H, m), 7.20(1H, m), 6.95(1H, m), 6.70(1H, m), 6.34(1H, m), 4.86(1H, s), 3.65(2H, m); ^{13}C NMR (400MHz, DMSO-d_6): δ= 169.62, 169.20, 162.02, 161.09, 159.10, 158.62, 141.91, 140.38, 134.32, 131.81, 131.31, 129.18, 129.11, 125.22, 123.33, 122.71, 120.63, 117.45, 116.67, 116.44, 116.12, 115.82, 113.99, 42.33ppm. HRMS (ESI) $(M+H)^+$ Calc'd for $C_{25}H_{21}FN_6O_3$: 473.1738 Found: 473.1736.

4.1.27.

N-(4-(2-((2-aminophenyl)amino)-2-oxoethyl)phenyl)-4-(2-methoxybenzamido)-1H-pyrazole-3-carboxamide (**14g**) Yield: 80%; HPLC Rt= 2.977min; ^{1}H NMR (400MHz,

DMSO-d_6): δ= 11.80(1H, s), 9.43(1H, s), 8.46(1H, s), 8.14(1H, m), 7.84(2H, d, *J*=8.42Hz), 7.59(1H, m), 7.36(2H, m), 7.26(1H, d, *J*=8.22Hz), 7.14(3H, m), 6.91(1H, m), 6.74(1H, m), 6.55(1H, m), 4.87(2H, s), 4.14(3H, s), 3.65(2H, s); ^{13}C NMR (400MHz, DMSO-d_6): δ= 169.74, 162.35, 161.47, 157.98, 142.40, 137.42, 134.11, 131.88, 129.72, 126.33, 125.77, 123.83, 123.50, 121.39, 120.90, 120.58, 116.63, 116.33, 112.85, 56.53, 42.64ppm. HRMS (ESI) $(M+H)^+$ Calc'd for $C_{26}H_{24}N_6O_4$: 485.1938 Found:485.1931.

General Procedure for the synthesis of **15a-15g**. A solution of KOH (2.84g, 50.6mmol) in MeOH (7mL) was added dropwise into a solution of hydroxylamine hydrochloride (2.34g, 33.7mmol) in MeOH (12mL) in an ice bath. The mixture was stirred at 0□ for 1h, and then was filtered to obtain a fresh solution of NH_2OH in MeOH. Then compound **13** (0.22mmol, 1equiv) was dissolved in 3mL of the aforementioned fresh solution of NH_2OH. The mixture was stirred for 1h at room temperature. TLC analysis (ethyl acetate: methanol=5:1) indicated the complete reaction. The reaction mixture was evaporated under reduced pressure, and was acidified with 2N HCl (pH at 5-6) to form precipitation. The precipitate was isolated by filtration and dried to afford the corresponding compounds **15a-15g** as a white solid.

4.1.28.
4-(2,6-dichlorobenzamido)-N-(4-(2-(hydroxyamino)-2-oxoethyl)phenyl)-1H-pyrazole-3-carboxamide (**15a**) Yield: 71%; HPLC Rt= 2.973min; ^{1}H NMR (400MHz, DMSO-d_6): δ= 10.66(1H, s), 10.30(1H, s), 10.16(1H, s), 8.83(1H, s), 8.44(1H, s), 7.71(2H, d, *J*=8.67Hz), 7.57(4H, m), 7.20(2H, d, *J*=8.18Hz), 3.24(2H, s); ^{13}C NMR (400MHz, DMSO-d_6): δ= 167.05, 160.68, 136.57, 135.47, 131.74, 131.48, 131.29, 128.96, 128.31, 121.66, 120.43ppm. HRMS (ESI) $(M+H)^+$ Calc'd for $C_{19}H_{15}Cl_2N_5O_4$: 448.0580 Found: 448.0573.

4.1.29.
4-(2-chloro-6-fluorobenzamido)-N-(4-(2-(hydroxyamino)-2-oxoethyl)phenyl)-1H-pyrazole-3-carboxamide (**15b**) Yield: 76%; HPLC Rt= 2.985min; ^{1}H NMR (400MHz, DMSO-d_6): δ= 13.64(1H, s), 10.69(1H, s), 10.31(2H, m), 8.86(1H, s), 8.46(1H, s), 7.74(2H, m), 7.58(1H, m), 7.45(2H, m), 7.23(2H, m), 3.27(2H, s); ^{13}C NMR (400MHz, DMSO-d_6): δ= 167.60, 162.19, 160.68, 159.09, 158.21, 137.09, 133.80, 132.73, 132.63, 131.97, 131.68, 129.47, 126.19, 122.17, 121.93, 120.95, 115.53, 115.31ppm. HRMS (ESI) $(M+H)^+$ Calc'd for $C_{19}H_{15}ClFN_5O_4$: 432.0876 Found: 432.0876.

4.1.30.
4-(2,6-difluorobenzamido)-N-(4-(2-(hydroxyamino)-2-oxoethyl)phenyl)-1H-pyrazole-3-carboxamide (**15c**) Yield: 78%; HPLC Rt= 2.977min; ^{1}H NMR (400MHz, DMSO-d_6): δ= 13.67(1H, s), 10.72(1H, s), 10.34(2H, m), 8.85(1H, s), 8.43(1H, s),

7.73(2H, m), 7.63(1H, m), 7.27(4H, m), 3.26(2H, s); ^{13}C NMR (400MHz, DMSO-d_6): δ= 167.57, 162.27, 160.99, 160.92, 158.50, 158.44, 156.94, 137.07, 133.65, 133.32, 132.00, 129.94, 129.49, 122.30, 121.78, 120.95, 114.24, 112.97, 112.73ppm. HRMS (ESI) $(M+H)^+$ Calc'd for $C_{19}H_{15}F_2N_5O_4$: 416.1171 Found: 416.1167.

4.1.31.
4-benzamido-N-(4-(2-(hydroxyamino)-2-oxoethyl)phenyl)-1H-pyrazole-3-carboxamide (**15d**) Yield: 87%; HPLC Rt= 2.982min; ^{1}H NMR (400MHz, DMSO-d_6): δ= 10.72(1H, s), 10.58(1H, m), 10.36(1H, m), 8.40(1H, s), 7.91(2H, m), 7.78(2H, m), 7.62(4H, m), 7.26(2H, m), 3.29(2H, s); ^{13}C NMR (400MHz, DMSO-d_6): δ= 167.58, 163.31, 136.98, 133.76, 132.62, 132.53, 132.13, 129.98, 129.53, 127.25, 123.63, 121.54, 121.21, ppm. HRMS (ESI) $(M+H)^+$ Calc'd for $C_{19}H_{17}N_5O_4$: 380.1360 Found:380.1354.

4.1.32.
4-(2-chlorobenzamido)-N-(4-(2-(hydroxyamino)-2-oxoethyl)phenyl)-1H-pyrazole-3-carboxamide (**15e**) Yield: 59%; HPLC Rt= 2.950min; ^{1}H NMR (400MHz, DMSO-d_6): δ= 13.61(1H, s), 10.69(1H, s), 10.32(1H, s), 10.21(1H, s), 8.43(1H, s), 7.73(3H, t, *J*=8.36Hz), 7.51(4H, m), 7.21(2H, d, *J*=8.34Hz), 3.26(2H, s); ^{13}C NMR (400MHz, DMSO-d_6): δ= 167.08, 162.57, 136.51, 134.80, 132.02, 131.53, 130.22, 129.92, 129.63, 128.99, 127.65, 122.38, 120.56ppm. HRMS (ESI) $(M+H)^+$ Calc'd for $C_{19}H_{16}ClN_5O_4$: 414.0970 Found: 414.0971.

4.1.33.
4-(2-fluorobenzamido)-N-(4-(2-(hydroxyamino)-2-oxoethyl)phenyl)-1H-pyrazole-3-carboxamide (**15f**) Yield: 63%; HPLC Rt= 2.965min; ^{1}H NMR (400MHz, DMSO-d_6): δ= 13.68(1H, s), 10.77(2H, m), 10.14(2H, m), 8.45(1H, s), 8.05(1H, m), 7.75(3H, m), 7.43(2H, m), 7.26(2H, d, *J*=8.51Hz), 3.29(2H, s); ^{13}C NMR (400MHz, DMSO-d_6): δ= 167.12, 161.07, 159.09, 158.61, 136.56, 134.34, 134.25, 131.54, 131.32, 129.05, 125.25, 125.22, 122.59, 120.54, 120.46, 120.34, 116.67, 116.43, 30.39ppm. HRMS (ESI) $(M+H)^+$ Calc'd for $C_{19}H_{16}FN_5O_4$: 398.1265 Found:398.1266.

4.1.34.
N-(4-(2-(hydroxyamino)-2-oxoethyl)phenyl)-4-(2-methoxybenzamido)-1H-pyrazole-3-carboxamide (**15g**) Yield: 70%; HPLC Rt= 2.988min; ^{1}H NMR (400MHz, DMSO-d_6): δ= 11.80(1H, s), 10.76(1H, s), 10.23(1H, m), 8.46(1H, m), 8.14(1H, d, *J*=7.53Hz), 7.83(2H, m), 7.60(1H, m), 7.28(5H, m), 4.15(3H, s), 3.30(2H, s); ^{13}C NMR (400MHz, DMSO-d_6): δ= 173.27, 167.65, 161.51, 157.98, 137.34, 134.14, 131.88, 130.01, 129.56, 123.50, 121.40, 121.19, 120.88, 120.52, 112.85, 56.53ppm. HRMS (ESI) $(M+H)^+$ Calc'd for $C_{20}H_{19}N_5O_5$: 410.1465 Found:410.1460.

4.1.35 ethyl 7-(4-(2,6-dichlorobenzamido)-1H-pyrazole-3-carboxamido)heptanoate (**16a**) Yield: 70%; A mixture of acid **12a** (1.67mmol, 1equiv), amine (1.67mmol, 1equiv), EDCI (2.00mmol, 1.2equiv), HOBt (2.00mmol, 1.2equiv) and DIEA

(4.01mmol, 2.4equiv) were mixed in DMF (20mL). TLC analysis, using ethyl acetate: petroleum ether (1:1) as the eluent, indicated the complete reaction. The mixture was diluted with water and then extracted with ethyl acetate. The organic layer was collected and dried by anhydrous sodium sulfate. The crude product was further purified by flash column chromatography with an appropriate ethyl acetate/petroleum ether mixture to provide the corresponding compound **16a**. ^{1}H NMR (400MHz, DMSO-d_6): δ=13.36(1H, s), 10.16(1H, s), 8.35(2H, m), 7.59 (3H, m), 4.05 (2H, m), 3.21 (2H, m), 2.24(2H, t, *J*=7.03Hz), 1.51 (4H, m), 1.25(4H, m),1.13(3H, t, *J*=7.40Hz); HRMS (ESI) $(M+H)^+$ Calc'd for $C_{20}H_{24}Cl_2N_4O_4$: 455.1254 Found:455.1257.

Compounds **16b-16g** were prepared according to a similar procedure described for **16a**.

General Procedure for the synthesis of **17a-17g**. A solution of KOH (2.84g, 50.6mmol) in MeOH (7mL) was added dropwise into a solution of hydroxylamine hydrochloride (2.34g, 33.7mmol) in MeOH (12mL) in an ice bath. The mixture was stirred at 0□ for 1h, and then was filtered to obtain a fresh solution of NH_2OH in MeOH. Then compound **16** (0.44mmol, 1equiv) was dissolved in 3mL of the aforementioned fresh solution of NH_2OH. The mixture was stirred for 1h at room temperature. TLC analysis (ethyl acetate: methanol=5:1) indicated the complete reaction. The reaction mixture was evaporated under reduced pressure, and was acidified with 2N HCl (pH at 5-6) to form precipitation. The precipitate was isolated by filtration and dried to afford the corresponding compounds **17a-17g**.

4.1.36.
4-(2,6-dichlorobenzamido)-N-(7-(hydroxyamino)-7-oxoheptyl)-1H-pyrazole-3-carboxamide (**17a**) Yield: 72%; HPLC Rt= 3.028min; ^{1}H NMR (400MHz, DMSO-d_6): δ= 13.43(1H, s), 10.38(1H, s), 10.20(1H, s), 8.48(1H, s), 8.37(1H, s), 7.58(4H, m), 3.22(2H, m), 1.95(2H, m), 1.49(4H, s), 1.26(4H, s); ^{13}C NMR (400MHz, DMSO-d_6): δ= 169.63, 163.55, 160.81, 135.83, 132.31, 131.73, 128.86, 121.83, 38.65, 32.68, 29.49, 28.77, 26.63, 25.56ppm. HRMS (ESI) $(M+H)^+$ Calc'd for $C_{18}H_{21}Cl_2N_5O_4$: 442.1050 Found:442.1046.

4.1.37.
4-(2,6-dichlorobenzamido)-N-(6-(hydroxyamino)-6-oxohexyl)-1H-pyrazole-3-carboxamide (**17b**) Yield: 74%; HPLC Rt= 3.048min; ^{1}H NMR (400MHz, DMSO-d_6): δ= 13.44(1H, s), 10.39(1H, s), 10.12(1H, s), 8.41(1H, s), 8.29(1H, s), 7.50(4H, m), 3.15(2H, m), 1.90(2H, m), 1.44(4H, m), 1.18(2H, m); ^{13}C NMR (400MHz, DMSO-d_6): δ= 174.90, 169.69, 163.62, 160.82, 135.80, 133.37, 132.30, 131.72, 128.85, 121.84, 121.11, 38.58, 32.65, 29.32, 26.49, 25.33ppm. HRMS (ESI) $(M+H)^+$ Calc'd for $C_{17}H_{19}Cl_2N_5O_4$: 428.0893 Found:428.0892.

4.1.38.
4-(2,6-difluorobenzamido)-N-(7-(hydroxyamino)-7-oxoheptyl)-1H-pyrazole-3-carbox

amide (**17c**) Yield: 75%; HPLC Rt= 3.055min; ^{1}H NMR (400MHz, DMSO-d_6): δ= 10.45(2H, s), 8.51(1H, s), 8.37(1H, s), 7.65(1H, m), 7.28(2H, m), 3.25(2H, m), 1.98(2H, m), 1.52(4H, s), 1.29(4H, s); ^{13}C NMR (400MHz, DMSO-d_6): δ= 174.94, 169.68, 163.55, 160.95, 158.46, 156.62, 133.42, 133.32, 133.22, 122.00, 112.97, 112.73, 38.64, 32.67, 29.51, 28.78, 26.62, 25.56ppm. HRMS (ESI) $(M+H)^+$ Calc'd for $C_{18}H_{21}F_2N_5O_4$: 410.1641 Found:410.1642.

4.1.39.
4-(2,6-difluorobenzamido)-N-(6-(hydroxyamino)-6-oxohexyl)-1H-pyrazole-3-carbox amide (**17d**) Yield: 65%; HPLC Rt= 3.020min; ^{1}H NMR (400MHz, DMSO-d_6): δ= 13.40(1H, s), 10.44(2H, m), 8.73(1H, s), 8.49(1H, m), 8.37(1H, s), 7.64(1H, m), 7.28(2H, m), 3.25(2H, m), 1.98(2H, m), 1.53(4H, m), 1.27(2H, m); ^{13}C NMR (400MHz, DMSO-d_6): δ= 169.61, 163.65, 160.95, 158.39, 156.61, 133.44, 133.34, 133.24, 121.97, 112.98, 112.74, 38.57, 32.67, 29.37, 26.49, 25.35ppm. HRMS (ESI) $(M+H)^+$ Calc'd for $C_{17}H_{19}F_2N_5O_4$: 396.1484 Found:396.1484.

4.1.40.
4-(2,6-difluorobenzamido)-N-(5-(hydroxyamino)-5-oxopentyl)-1H-pyrazole-3-carbox amide (**17e**) Yield: 59%; HPLC Rt= 3.013min; ^{1}H NMR (400MHz, DMSO-d_6): δ= 13.38(1H, s), 10.41(1H, s), 10.35(1H, s), 8.67(1H, s), 8.50(1H, m), 8.34(1H, s), 7.63(1H, m), 7.27(2H, t, *J*=8.20Hz), 3.21(2H, m), 1.97(2H, m), 1.50(4H, m); ^{13}C NMR (400MHz, DMSO-d_6): δ= 169.46, 163.70, 160.94, 158.39, 156.56, 133.48, 133.38, 121.96, 121.08, 113.01, 112.77, 38.36, 32.46, 29.28, 23.13ppm. HRMS (ESI) $(M+H)^+$ Calc'd for $C_{16}H_{17}F_2N_5O_4$: 382.1328 Found:382.1328.

4.1.41.
4-(2,6-difluorobenzamido)-N-(4-(hydroxyamino)-4-oxobutyl)-1H-pyrazole-3-carboxa mide (**17f**) Yield: 56%; HPLC Rt= 2.990min; ^{1}H NMR (400MHz, DMSO-d_6): δ= 13.38(1H, s), 10.39(2H, d, *J*=8.25Hz), 8.69(1H, s), 8.54(1H, m), 8.34(1H, s), 7.63(1H, m), 7.27(2H, t, *J*=8.46Hz), 3.24(2H, m), 1.98(2H, t, *J*=7.62Hz), 1.73(2H, m); ^{13}C NMR (400MHz, DMSO-d_6): δ= 169.22, 163.79, 160.88, 158.40, 156.57, 133.39, 133.31, 121.98, 121.09, 113.02, 112.78, 38.37, 30.45, 25.88ppm. HRMS (ESI) $(M+H)^+$ Calc'd for $C_{15}H_{15}F_2N_5O_4$: 368.1171 Found:368.1173.

4.1.42.
4-(2-chloro-6-fluorobenzamido)-N-(7-(hydroxyamino)-7-oxoheptyl)-1H-pyrazole-3-c arboxamide (**17g**) Yield: 54%; HPLC Rt= 2.943min; ^{1}H NMR (400MHz, DMSO-d_6): δ= 10.35(1H, s), 8.51(1H, s), 8.35(1H, s), 7.57(1H, m), 7.46(1H, d, *J*=8.09Hz), 7.39(1H, t, *J*=8.88Hz), 3.21(2H, m), 1.94(2H, t, *J*=7.39Hz), 1.48(4H, m), 1.25(4H, m); ^{13}C NMR (400MHz, DMSO-d_6): δ= 169.52, 163.49, 160.61, 158.72, 158.14, 133.03, 132.76, 131.63, 126.28, 121.96, 115.57, 115.36, 38.64, 32.67, 29.50, 28.78, 26.63, 25.56ppm. HRMS (ESI) $(M+H)^+$ Calc'd for $C_{18}H_{21}ClFN_5O_4$: 426,1345 Found:426.1347.

4.2 Biological evaluation

4.2.1 Cell antiproliferative activity assay

Human colorectal cancer cell line (HCT116), human lung cancer cell line (H460), human malignant melanoma cancer cell line (A375), human cervical cancer cell line (Hela) and human hepatoma cancer cell line (SMMC7721) were used in the current researches. We also selected the mouse embryonic fibroblast cells as the normal cells for cytotoxicity assays. The cell lines were grown in Dulbecco's Modified Eagle Medium (DMEM) containing 10% fetal bovine serum (FBS) (ThermoFisher, USA) and 1% penicillin/streptomycin at 37□, 5%CO_2 atmosphere. The cells were seeded into 96-well plates at a density of 4×10^3 cells / well. After 12h, the cells were treated with 10μL of various concentrations of compounds for 72h. Then 10μL per well of CCK-8 reagent were added, followed incubation for another 1h. The absorbance was measured at 450nm using an EnSpire multimode plate reader (PerkinElmer, USA).

4.2.2 *In vitro* HDAC inhibition assay

HDAC1 (BML-AK511), HDAC2 (BML-AK512), HDAC3 (BML-AK531), HDAC6 (BML-AK516) and HDAC8 (BML-AK518) were purchased by Enzo Life Sciences Inc. According to the instructions, various concentrations of the tested compounds (10μL) and HDAC enzyme solution (15μL) were mixed into a 96-well microplate. The mixture was cultured at 37□ for 10min. Then 25μL of diluted HDAC substrate was added to start the deacetylation reaction at 37□ for 30min.Then 50μL of 1x developer was added, and the mixture was incubated at 37□ for 20min, which stopped the reaction. Fluorescence was analyzed using an EnSpire multimode plate reader (PerkinElmer, USA).

4.2.3 *In vitro* CDK inhibition assay

The CDK1, 2, 4, 6 and 7 inhibitory activity were measured by CDK1/ Cyclin A2 Kinase Enzyme System (Promega Catalog # V2961), CDK2/ Cyclin A2 Kinase Enzyme System (Promega Catalog # V2971), CDK4/ Cyclin D1 Kinase Enzyme System (CDK4/Cyclin D1, Active Catalog No. C31-10G signalchem), CDK6/ Cyclin D3 Kinase Enzyme System (Promega Catalog # V4510), and CDK7/ Cyclin H1 Kinase Enzyme System (CDK7/ Cyclin H1 , Active Catalog No. C36-102H signalchem), respectively. The kinase reaction mixture contained 1μL of the tested compound, 2μL of enzyme, and 2μL of 2.5 x ATP/substrate mix. After incubation at room temperature for 10min, the reaction was stopped by adding 5μL of ADP□Glo™ Reagent. Forty minutes later, 10μL of Kinase Detection Reagent was added, and the plate was incubated at room temperature for 30min. Luminescence was recorded by an EnSpire multimode plate reader (PerkinElmer, USA).

4.2.4 Molecular docking

The three-dimensional structures of HDAC2 (PDB code: 4LXZ) and CDK2 (PDB code: 1PYE) were performed from the Protein Data Bank. The molecular docking was carried out via Surflexdock in Sybyl-X 2.0 (Tripos Inc.). The water and ligands were removed and the polar hydrogens were added to the protein structure. The molecular structures of tested compounds **7c** and **14a** were optimized with Tripos force field. Then compounds **7c** and **14a** were docked into HDAC2 and CDK2 using Surflex-Dock module.

4.2.5 Cell migration assay

A375 or H460 cells were plated in a 12-well plate at a density of 1.0×10^4 cells / well. Twelve hours later, a straight line was scratched at the bottom of each well using a 10μL pipette tip. After washing with phosphate-buffered saline (PBS), A375 cells (H460 cells) were treated with compounds **7c** and **14a** at the concentration of 0.25μM (0.5μM). Then cells were cultured for 48h. The cell images were captured by an OPTEC BDS200 microscope.

4.2.6 Cell cycle analysis

The different cells were plate in 6-well plates at a density of 1.0×10^6 cells / well. Twelve hours later, 20μL of compounds **7c**, **14a**, **1** and CS055 were added into 6 wells at the concentrations of 2, 1 and 0.5μM respectively for 24h. Then cells were harvested, washed with phosphate-buffered saline (PBS), and fixed in cold 75% ethanol at -20□ for 24h. After adding 200μL of RNase A, cells were incubated at 37°C for 30min, and then stained with 200μL of propidium iodide (PI) at 4°C for 30min. Cells were screened by the flow cytometry.

4.2.7 Cell apoptosis assay

The different cells were plated in 6-well plates at a density of 1.0×10^6 cells / well. Twelve hours later, 20μL of compounds **7c**, **14a**, **1** and CS055 were added into 6 wells at the concentrations of 2, 1 and 0.5μM respectively for 48h. Then cells were harvested, washed with phosphate-buffered saline (PBS), and resuspended in 500μL of 1 X annexin-binding buffer. The resuspended cells were stained with 5μL of Annexin V-FITC (10 mg/ml) and 2μL of propidium iodide in the dark for 15min. Cells were detected by the flow cytometry.

4.2.8 Immunofluorometric assay

A375 cells were plated into confocal dishes with 8.0×10^3 cells / well. Twelve hours later, 20μL of compounds **7c** and **14a** were added into dishes at the concentration of 1μM for 12h respectively. Then cells were washed with phosphate-buffered saline (PBS), and fixed with 4% paraformaldehyde. Thirty

minutes later, cells were permeabilized with 0.3% Triton X-100, and incubated in 3% bovine serum albumin (BSA) for 1h. Then cells were treated with the diluted primary antibody (anti-Histone H3 (acetyl K9)) overnight at 4□, and incubated with the secondary antibody (IgG H&L (Alexa Fluor® 488)) for 2h in the dark. After adding DAPI, the cells were cultured at room temperature for 3min in the dark. The samples were analyzed by Leica TCS SP8 confocal fluorescence microscope (Leica Microsystems, Germany). For the immunofluorometric assay of CDK2 in A375 cells treated with compounds **7c** and **14a**, cells were fixed with 4% paraformaldehyde, permeabilized with 0.3% Triton X-100, and incubated in 3% bovine serum albumin (BSA). One hour later, the cells were incubated with anti-CDK2 antibody (Alexa Fluor® 488) overnight at 4□, and then were stained with DAPI for 3min. The samples were analyzed by Leica TCS SP8 confocal fluorescence microscope (Leica Microsystems, Germany).

4.2.9 ROS accumulation assay

A375 cells were plated into confocal dishes with 1.0×10^6 cells / well. Twelve hours later, 20μL of compounds **7c** and **14a** were added into dishes at the concentration of 1μM for 12h respectively. The cells were washed with phosphate-buffered saline (PBS), and incubated with 1μL of DCFH-DA at 37°C for 0.5h. Then the cells were washed with PBS three times, and analyzed by Leica TCS-SP8 confocal fluorescence microscope (Leica Microsystems, Germany).

4.2.10 Pharmacokinetic parameters

The pharmacokinetic properties (PK) were carried out in ICR male mice, by administering **7c** and **14a** intraperitoneally (IP) at a dose of 20mg/kg respectively. Compounds **7c** and **14a** were dissolved in a solution of DMSO: CrEL: Saline=10:10:80 (v/v/v). The blood samples were collected at 0.25h, 0.5h, 1h, 2h, 4h, 8h, 12h and 24h after intraperitoneal injection, and then analyzed by LC-MS/MS system. The PK parameters were estimated by noncompartmental model using WinNonlin 8.0.

4.2.11 *In vivo* antitumor activity assay

All animal experiments were approved by the local ethics committee. BALB/c nude female mice (5-6 weeks old) were afforded by Vital River Laboratory Animal Technology Co. Ltd. To establish HCT116 xenograft models, 3×10^6 human colorectal cancer cells were subcutaneously injected into the front-right axilla region of nude mice. When tumors grew to a volume of 100-300 mm^3, the BALB/c female mice were randomly divided into treatment and control groups (6 mice per group). Mice in the treatment groups were intraperitoneally injected with compound **7c** at a dose of 12.5mg/kg and 25mg/kg once daily (QD) for 21 days respectively, and mice in the

control group were injected with equal volume of 0.5% MC aqueous solution. During treatment, tumor volumes and body weighs were measured every 3 days. The tumor growth inhibition (TGI) was calculated according to the following formula: TGI $=100\%\times[1-(TV_{t(T)}-TV_{initial(T)})/(TV_{t(C)}-TV_{initial(C)})]$, where $TV_{t(T)}$ and $TV_{initial(T)}$ are the tumor volume measured at initial time and final time of treatment in the treatment group respectively, and $TV_{t(C)}$ and $TV_{initial(C)}$ are the tumor volume for the control group.

Acknowledgments

We are grateful to the National Natural Science Foundation of China (Grant No. 21176018) for their generous financial supports.

Appendix A. Supplementary data

Supplementary data related to this article can be found at xxxxx.

Reference

[1] S.J. Conway, P.M. Woster, W.J. Greenlee, G. Georg, S. Wang, Epigenetics: Novel Therapeutics Targeting Epigenetics, Journal of Medicinal Chemistry, 59 (2016) 1247-1248.

[2] S. Ropero, M. Esteller, The role of histone deacetylases (HDACs) in human cancer, Molecular Oncology, 1 (2007) 19-25.

[3] T. Kouzarides, Chromatin Modifications and Their Function, Cell, 128 (2007) 693-705.

[4] O. Witt, H.E. Deubzer, T. Milde, I. Oehme, HDAC family: What are the cancer relevant targets?, Cancer Letters, 277 (2009) 8-21.

[5] Mark A. Dawson, T. Kouzarides, Cancer Epigenetics: From Mechanism to Therapy, Cell, 150 (2012) 12-27.

[6] A. Moran, R. Katz, N.S. Jenny, B. Astor, D.A. Bluemke, J.A.C. Lima, D. Siscovick, A.G. Bertoni, M.G. Shlipak, Left Ventricular Hypertrophy in Mild and Moderate Reduction in Kidney Function Determined Using Cardiac Magnetic Resonance Imaging and Cystatin C: The Multi-Ethnic Study of Atherosclerosis (MESA), American Journal of Kidney Diseases, 52 (2008) 839-848.

[7] A.C. West, R.W. Johnstone, New and emerging HDAC inhibitors for cancer treatment, J Clin Invest, 124 (2014) 30-39.

[8] D.A. Rodrigues, G.À. Ferreira-Silva, A.C.S. Ferreira, R.A. Fernandes, J.K. Kwee, C.M.R. Sant'Anna, M. Ionta, C.A.M. Fraga, Design, Synthesis, and Pharmacological Evaluation of Novel N-Acylhydrazone Derivatives as Potent Histone Deacetylase 6/8 Dual Inhibitors, Journal of Medicinal Chemistry, 59 (2016) 655-670.

[9] M. Haberland, R.L. Montgomery, E.N. Olson, The many roles of histone deacetylases in development and physiology: implications for disease and therapy, Nature Reviews Genetics, 10 (2009) 32-42.

[10] P.A. Marks, Discovery and development of SAHA as an anticancer agent, Oncogene, 26 (2007) 1351.

[11] C. Grant, F. Rahman, R. Piekarz, C. Peer, R. Frye, R.W. Robey, E.R. Gardner, W.D. Figg, S.E.

Bates, Romidepsin: a new therapy for cutaneous T-cell lymphoma and a potential therapy for solid tumors, Expert Review of Anticancer Therapy, 10 (2010) 997-1008.

[12] A.C. Rashidi, A.F., Belinostat for the treatment of relapsed or refractory peripheral T-cell lymphoma, Future Oncol., 11 (2015) 1659-1664.

[13] S.L. Greig, Panobinostat: A Review in Relapsed or Refractory Multiple Myeloma, Targeted Oncology, 11 (2016) 107-114.

[14] G. Shuai, L. Xiaoyang, Z. Jie, X. Wenfang, Z. Yingjie, Preclinical and Clinical Studies of Chidamide (CS055/HBI-8000), An Orally Available Subtype-selective HDAC Inhibitor for Cancer Therapy, Anti-Cancer Agents in Medicinal Chemistry, 17 (2017) 802-812.

[15] D. Hanahan, Robert A. Weinberg, Hallmarks of Cancer: The Next Generation, Cell, 144 (2011) 646-674.

[16] S.C. Jiahuai Tan, Yuehua Ma, Richard L Petrillo, Delong Liu, Novel histone deacetylase inhibitors in clinical trials as anti-cancer agents, Journal of Hematology & Oncology 3(2010) 5.

[17] H.D.S.a.S. Nuyts, Radiosensitizing Potential of Epigenetic Anticancer Drugs, Anti-Cancer Agents in Medicinal Chemistry, 9 (2009) 99-108.

[18] M. Bots, R.W. Johnstone, Rational combinations using HDAC inhibitors, Clinical cancer research : an official journal of the American Association for Cancer Research, 15 (2009) 3970-3977.

[19] A. Anighoro, J. Bajorath, G. Rastelli, Polypharmacology: Challenges and Opportunities in Drug Discovery, Journal of Medicinal Chemistry, 57 (2014) 7874-7887.

[20] N.M.O.B.a.M.J. Meegan, Designed Multiple Ligands for Cancer Therapy, Current Medicinal Chemistry, 18 (2011) 4722-4737.

[21] R. Morphy, C. Kay, Z. Rankovic, From magic bullets to designed multiple ligands, Drug Discovery Today, 9 (2004) 641-651.

[22] T.M. Sielecki, J.F. Boylan, P.A. Benfield, G.L. Trainor, Cyclin-Dependent Kinase Inhibitors: Useful Targets in Cell Cycle Regulation, Journal of Medicinal Chemistry, 43 (2000) 1-18.

[23] N. P, Genetic-control of cell-size at cell division in yeast, Nature, 256 (1975) 547-551.

[24] A. Errico, K. Deshmukh, Y. Tanaka, A. Pozniakovsky, T. Hunt, Identification of substrates for cyclin dependent kinases, Advances in Enzyme Regulation, 50 (2010) 375-399.

[25] U. Asghar, A.K. Witkiewicz, N.C. Turner, E.S. Knudsen, The history and future of targeting cyclin-dependent kinases in cancer therapy, Nature reviews. Drug discovery, 14 (2015) 130-146.

[26] M.S. Ingham, G. K., Cell-cycle therapeutics come of age, Journal of Clinical Oncology, 35 (2017) 2949-2959.

[27] S.B. Bharate, V. Kumar, S.K. Jain, M.J. Mintoo, S.K. Guru, V.K. Nuthakki, M. Sharma, S.S. Bharate, S.G. Gandhi, D.M. Mondhe, S. Bhushan, R.A. Vishwakarma, Discovery and Preclinical Development of IIIM-290, an Orally Active Potent Cyclin-Dependent Kinase Inhibitor, Journal of Medicinal Chemistry, 61 (2018) 1664-1687.

[28] E. Estey, H. Döhner, Acute myeloid leukaemia, The Lancet, 368 (2006) 1894-1907.

[29] Y. Wang, Y. Zhi, Q. Jin, S. Lu, G. Lin, H. Yuan, T. Yang, Z. Wang, C. Yao, J. Ling, H. Guo, T. Li, J. Jin, B. Li, L. Zhang, Y. Chen, T. Lu, Discovery of 4-((7H-Pyrrolo[2,3-d]pyrimidin-4-yl)amino)-N-(4-((4-methylpiperazin-1-yl)methyl)phenyl)-1H-pyrazole-3-carboxamide (FN-1501), an FLT3- and CDK-Kinase Inhibitor with Potentially High Efficiency against Acute Myelocytic Leukemia, Journal of Medicinal Chemistry, 61 (2018) 1499-1518.

[30] S. Wang, G. Griffiths, C.A. Midgley, A.L. Barnett, M. Cooper, J. Grabarek, L. Ingram, W. Jackson, G. Kontopidis, S.J. McClue, C. McInnes, J. McLachlan, C. Meades, M. Mezna, I. Stuart, M.P. Thomas,

D.I. Zheleva, D.P. Lane, R.C. Jackson, D.M. Glover, D.G. Blake, P.M. Fischer, Discovery and Characterization of 2-Anilino-4- (Thiazol-5-yl)Pyrimidine Transcriptional CDK Inhibitors as Anticancer Agents, Chemistry & Biology, 17 (2010) 1111-1121.

[31] R.P. Palanisamy, Palbociclib: A new hope in the treatment of breast cancer, Journal of cancer research and therapeutics, 12 (2016) 1220-1223.

[32] B. Laderian, T. Fojo, CDK4/6 Inhibition as a therapeutic strategy in breast cancer: palbociclib, ribociclib, and abemaciclib, Seminars in Oncology, 44 (2017) 395-403.

[33] W. Cheng, Z. Yang, S. Wang, Y. Li, H. Wei, X. Tian, Q. Kan, Recent development of CDK inhibitors: An overview of CDK/inhibitor co-crystal structures, European Journal of Medicinal Chemistry, 164 (2019) 615-639.

[34] J. Cicenas, K. Kalyan, A. Sorokinas, E. Stankunas, J. Levy, I. Meskinyte, V. Stankevicius, A. Kaupinis, M. Valius, Roscovitine in cancer and other diseases, Annals of translational medicine, 3 (2015) 135.

[35] P.G. Wyatt, A.J. Woodhead, V. Berdini, J.A. Boulstridge, M.G. Carr, D.M. Cross, D.J. Davis, L.A. Devine, T.R. Early, R.E. Feltell, E.J. Lewis, R.L. McMenamin, E.F. Navarro, M.A. O'Brien, M. O'Reilly, M. Reule, G. Saxty, L.C.A. Seavers, D.-M. Smith, M.S. Squires, G. Trewartha, M.T. Walker, A.J.A. Woolford, Identification of N-(4-Piperidinyl)-4-(2,6-dichlorobenzoylamino)-1H-pyrazole-3-carboxamide (AT7519), a Novel Cyclin Dependent Kinase Inhibitor Using Fragment-Based X-Ray Crystallography and Structure Based Drug Design, Journal of Medicinal Chemistry, 51 (2008) 4986-4999.

[36] A.M.S. Vyomesh Patel, Decio Pinto, Jr., Tadashi Igishi, Mark Raffeld, Leticia Quintanilla-Martinez, John F. Ensley, Edward A. Sausville, and J. Silvio Gutkind, Flavopiridol, a Novel Cyclin-dependent Kinase Inhibitor, Suppresses the Growth of Head and Neck Squamous Cell Carcinomas by Inducing Apoptosis, The Journal of Clinical Investigation, 102 (1998) 1674-1681.

[37] P.L. Toogood, P.J. Harvey, J.T. Repine, D.J. Sheehan, S.N. VanderWel, H. Zhou, P.R. Keller, D.J. McNamara, D. Sherry, T. Zhu, J. Brodfuehrer, C. Choi, M.R. Barvian, D.W. Fry, Discovery of a Potent and Selective Inhibitor of Cyclin-Dependent Kinase 4/6, Journal of Medicinal Chemistry, 48 (2005) 2388-2406.

[38] J. Almenara, R. Rosato, S. Grant, Synergistic induction of mitochondrial damage and apoptosis in human leukemia cells by flavopiridol and the histone deacetylase inhibitor suberoylanilide hydroxamic acid (SAHA), Leukemia, 16 (2002) 1331-1343.

[39] J.M. Huang, M.A. Sheard, L. Ji, R. Sposto, N. Keshelava, Combination of vorinostat and flavopiridol is selectively cytotoxic to multidrug-resistant neuroblastoma cell lines with mutant TP53, Molecular cancer therapeutics, 9 (2010) 3289-3301.

[40] Y. Li, X. Luo, Q. Guo, Y. Nie, T. Wang, C. Zhang, Z. Huang, X. Wang, Y. Liu, Y. Chen, J. Zheng, S. Yang, Y. Fan, R. Xiang, Discovery of N1-(4-((7-Cyclopentyl-6-(dimethylcarbamoyl)-7H-pyrrolo[2,3-d]pyrimidin-2-yl)amino)phenyl)-N8-hydroxyoctanediamide as a Novel Inhibitor Targeting Cyclin-dependent Kinase 4/9 (CDK4/9) and Histone Deacetlyase1 (HDAC1) against Malignant Cancer, Journal of Medicinal Chemistry, 61 (2018) 3166-3192.

[41] A. Mai, S. Massa, D. Rotili, R. Pezzi, P. Bottoni, R. Scatena, J. Meraner, G. Brosch, Exploring the connection unit in the HDAC inhibitor pharmacophore model: Novel uracil-based hydroxamates, Bioorganic & Medicinal Chemistry Letters, 15 (2005) 4656-4661.

[42] T. Abdizadeh, M.R. Kalani, K. Abnous, Z. Tayarani-Najaran, B.Z. Khashyarmanesh, R. Abdizadeh,

R. Ghodsi, F. Hadizadeh, Design, synthesis and biological evaluation of novel coumarin-based benzamides as potent histone deacetylase inhibitors and anticancer agents, European Journal of Medicinal Chemistry, 132 (2017) 42-62.

[43] F. Canduri, H.B. Uchoa, W.F. de Azevedo, Jr., Molecular models of cyclin-dependent kinase 1 complexed with inhibitors, Biochemical and biophysical research communications, 324 (2004) 661-666.

[44] K.H. Oudah, M.A.A. Najm, N. Samir, R.A.T. Serya, K.A.M. Abouzid, Design, synthesis and molecular docking of novel pyrazolo[1,5-a][1,3,5]triazine derivatives as CDK2 inhibitors, Bioorganic Chemistry, 92 (2019) 103239.

[45] A. Deep, R.K. Marwaha, M.G. Marwaha, Jyoti, R. Nandal, A.K. Sharma, Flavopiridol as cyclin dependent kinase (CDK) inhibitor: a review, New Journal of Chemistry, 42 (2018) 18500-18507.

[46] S. Yoon, G.H. Eom, HDAC and HDAC Inhibitor: From Cancer to Cardiovascular Diseases, Chonnam medical journal, 52 (2016) 1-11.

[47] T. Kiesslich, D. Neureiter, HDAC inhibitors in liver cancer: which route to take?, Expert review of gastroenterology & hepatology, 13 (2019) 515-517.

[48] J. Zhao, S.G. Gray, C.M. Greene, M.W. Lawless, Unmasking the pathological and therapeutic potential of histone deacetylases for liver cancer, Expert review of gastroenterology & hepatology, 13 (2019) 247-256.

[49] W. Weichert, A. Roske, V. Gekeler, T. Beckers, C. Stephan, K. Jung, F.R. Fritzsche, S. Niesporek, C. Denkert, M. Dietel, G. Kristiansen, Histone deacetylases 1, 2 and 3 are highly expressed in prostate cancer and HDAC2 expression is associated with shorter PSA relapse time after radical prostatectomy, British journal of cancer, 98 (2008) 604-610.

[50] G. Eot-Houllier, G. Fulcrand, L. Magnaghi-Jaulin, C. Jaulin, Histone deacetylase inhibitors and genomic instability, Cancer Letters, 274 (2009) 169-176.

[51] P.C. Diao, W.Y. Lin, X.E. Jian, Y.H. Li, W.W. You, P.L. Zhao, Discovery of novel pyrimidine-based benzothiazole derivatives as potent cyclin-dependent kinase 2 inhibitors with anticancer activity, Eur J Med Chem, 179 (2019) 196-207.

[52] R. Jorda, L. Havlicek, A. Sturc, D. Tuskova, L. Daumova, M. Alam, J. Skerlova, M. Nekardova, M. Perina, T. Pospisil, J. Siroka, L. Urbanek, P. Pachl, P. Rezacova, M. Strnad, P. Klener, V. Krystof, 3,5,7-Substituted Pyrazolo[4,3- d]pyrimidine Inhibitors of Cyclin-Dependent Kinases and Their Evaluation in Lymphoma Models, J Med Chem, 62 (2019) 4606-4623.

[53] S. Tadesse, E.C. Caldon, W. Tilley, S. Wang, Cyclin-Dependent Kinase 2 Inhibitors in Cancer Therapy: An Update, J Med Chem, 62 (2019) 4233-4251.

[54] S. Kalra, G. Joshi, A. Munshi, R. Kumar, Structural insights of cyclin dependent kinases: Implications in design of selective inhibitors, Eur J Med Chem, 142 (2017) 424-458.

[55] Y. Ling, W.J. Gao, C. Ling, J. Liu, C. Meng, J. Qian, S. Liu, H. Gan, H. Wu, J. Tao, H. Dai, Y. Zhang, beta-Carboline and N-hydroxycinnamamide hybrids as anticancer agents for drug-resistant hepatocellular carcinoma, Eur J Med Chem, 168 (2019) 515-526.

[56] X. Chen, S. Zhao, H. Li, X. Wang, A. Geng, H. Cui, T. Lu, Y. Chen, Y. Zhu, Design, synthesis and biological evaluation of novel isoindolinone derivatives as potent histone deacetylase inhibitors, Eur J Med Chem, 168 (2019) 110-122.

[57] R. Sangwan, R. Rajan, P.K. Mandal, HDAC as onco target: Reviewing the synthetic approaches with SAR study of their inhibitors, Eur J Med Chem, 158 (2018) 620-706.

[58] A.B. Farag, H.A. Ewida, M.S. Ahmed, Design, synthesis, and biological evaluation of novel amide

and hydrazide based thioether analogs targeting Histone deacteylase (HDAC) enzymes, Eur J Med Chem, 148 (2018) 73-85.

[59] Y. Ling, J. Guo, Q. Yang, P. Zhu, J. Miao, W. Gao, Y. Peng, J. Yang, K. Xu, B. Xiong, G. Liu, J. Tao, L. Luo, Q. Zhu, Y. Zhang, Development of novel beta-carboline-based hydroxamate derivatives as HDAC inhibitors with antiproliferative and antimetastatic activities in human cancer cells, Eur J Med Chem, 144 (2018) 398-409.

[60] X. Li, Y. Zhang, Y. Jiang, J. Wu, E.S. Inks, C.J. Chou, S. Gao, J. Hou, Q. Ding, J. Li, X. Wang, Y. Huang, W. Xu, Selective HDAC inhibitors with potent oral activity against leukemia and colorectal cancer: Design, structure-activity relationship and anti-tumor activity study, Eur J Med Chem, 134 (2017) 185-206.

[61] X. Wu, X. Li, Z. Li, Y. Yu, Q. You, X. Zhang, Discovery of Nonquinone Substrates for NAD(P)H: Quinone Oxidoreductase 1 (NQO1) as Effective Intracellular ROS Generators for the Treatment of Drug-Resistant Non-Small-Cell Lung Cancer, Journal of Medicinal Chemistry, 61 (2018) 11280-11297.

[62] C. Gorrini, I.S. Harris, T.W. Mak, Modulation of oxidative stress as an anticancer strategy, Nature reviews. Drug discovery, 12 (2013) 931-947.

Highlights

1.A series of novel 1-H-pyrazole-3-carboxamide-based derivatives were designed and synthesized as histone deacetylase (HDAC) and cyclin-dependent kinase (CDK) dual inhibitors.

2. Compounds **7c** and **14a** exhibited excellent antiproliferative activities against HCT116 cells, A375 cells, Hela cells, H460 cells and SMMC7721 cells.

3. Compounds **7c** and **14a** showed potent inhibitory activity against HDAC and CDK.

4. Compounds **7c** and **14a** could arrest cell cycle in G2/M phase and promote apoptosis.

5. Compound **7c** possessed better pharmacokinetic properties compared with **14a**.

6. Compound **7c** exhibited potent antitumor efficacy in the HCT116 xenograft model (TGI= 51.0%).

Declaration of interests

☒ The authors declare that they have no known competing financial interests or personal relationships that could have appeared to influence the work reported in this paper.

☐The authors declare the following financial interests/personal relationships which may be considered as potential competing interests: